CHANGING CONTRIBUTION OF SNOW TO HUDSON BAY RIVER DISCHARGE

by

Bunu Sharma

M.Sc., Tribhuvan University, 2012

THESIS SUBMITTED IN PARTIAL FULFILLMENT OF
THE REQUIREMENTS FOR THE DEGREE OF
MASTER OF SCIENCE
IN
NATURAL RESOURCES AND ENVIRONMENTAL STUDIES
(ENVIRONMENTAL SCIENCE)

UNIVERSITY OF NORTHERN BRITISH COLUMBIA

April 2016

Abstract

Hudson Bay (HB) in northern Canada has experienced changing volumes and seasonality of streamflows in the last 100 years. These shifts may be due to changing snow accumulation and ablation regimes. This study quantifies the changing contribution of snow to river discharge from 20 major river basins draining into HB (including James Bay) between 1980 and 2013. The analysis is based on daily snow water equivalent (SWE) data from GlobSnow, and daily streamflow data from the Water Survey of Canada, Hydro-Québec, and Le Centre d'Expertise Hydrique du Québec. The contribution of snowmelt to streamflow generation is estimated from the ratio of water year maximum SWE to runoff. The Mann-Kendall test is performed for evaluation of trends and their significance. In HB, the snowmelt contribution to streamflow generation during 1980 to 2013 decreased by 15.9% $(34\ yr)^{-1}$ and changes in hydrological conditions are observed. The potential impacts of these changes on ecological and socio-economic systems across much of Canada's North are discussed.

Table of Contents

List of Tables

List of Figures

Acknowledgements

This thesis is an outcome of continuous guidance, suggestions and support from many people to whom I am greatly indebted. First and foremost, I would like to thank sincerely my supervisor, Dr. Stephen Déry, for letting me work under his supervision. His guidance, encouragement, inspiration, and continuous support has greatly influenced my study and research. I also wish to thank my committee members, Dr. Phil Owens and Dr. Gary Wilson, for their valuable comments on this work. I am also thankful to Dr. Chris Derksen for his invaluable suggestions on this research. I would like to thank Dr. Asa Rennermalm, Rutgers University for her valuable comments and suggestions on this work.

I would like to acknowledge the Natural Sciences and Engineering Research Council of Canada for funding this research, the University of Northern British Columbia (UNBC), the International Arctic Science Committee, and the Canadian Meteorological and Oceanographic Society for providing travel grants to attend conferences.

Thanks to the European Space Agency, Environment Canada, Hydro-Québec, Water Survey of Canada, Centre d'Expertise Hydrique du Québec, and Canadian Meterological Centre, for providing access to data.

I would like to give a special thanks to David Hah for compiling the updated streamflow data for this research and Dr. Siraj ul Islam for helping with data extraction. Many thanks to all of my colleagues and the members of the Northern Hydrometeorology Group (NHG) at UNBC for their generous support and the suggestions they provided at different times during this research.

I would not have finished this thesis if there had not been continuous support and inspiration of my dear husband Aseem Raj Sharma who helped me to fix R problems during my data analysis and complete overall writings.

I am obliged to my supportive family and friends for showering me with immense love, care and motivation to complete this work.

Lastly, I would like to dedicate this thesis with a special feeling of gratitude to my loving parents for their endless love, support and encouragement.

1. Introduction

1.1. Overview

Snow plays an important role in the generation of streamflow globally (Barnett, Adam, & Lettenmaier, 2005). The land surface water cycle over much of the global land area, poleward of about 40° latitude in both hemispheres, is dominated by snow accumulation and ablation processes (Adam, Hamlet, & Lettenmaier, 2009). As an example, Figure 1 shows the ratio of accumulated snowfall to annual runoff on a global scale. It emphasizes the critical role of snow processes to the hydrology of much of the global land area. Snow processes are therefore critical to water resources and economies globally (Adam et al., 2009; Barnett et al., 2005).

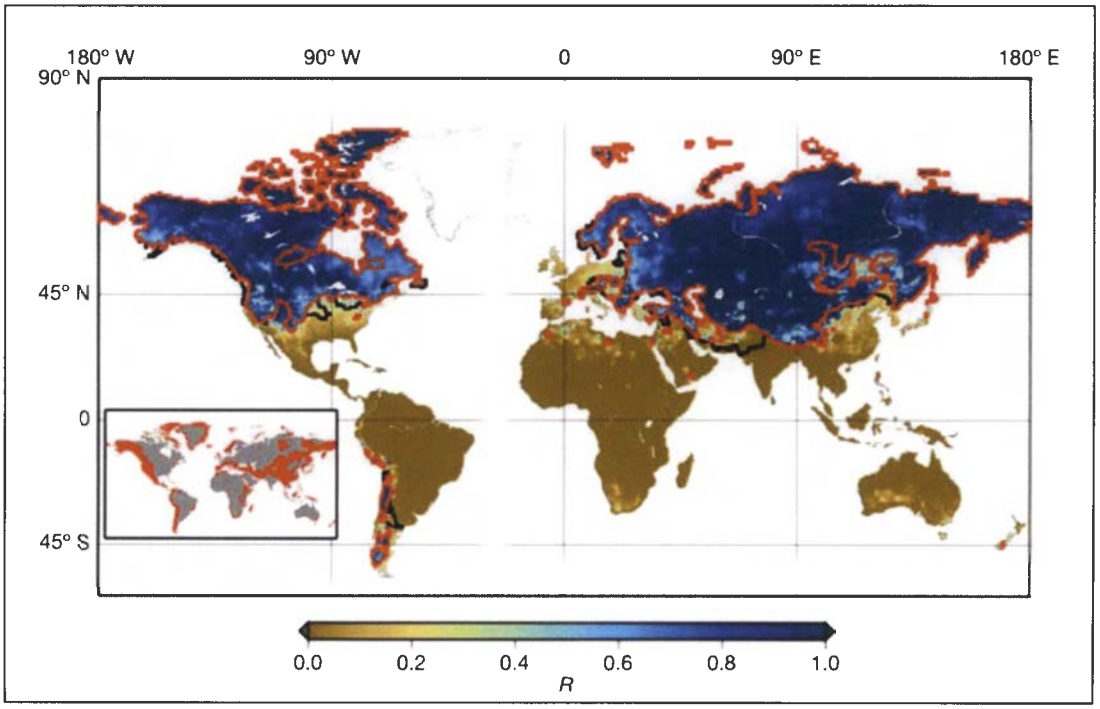

Figure 1. The importance of snowmelt-derived streamflow globally as illustrated by the ratio of accumulated annual snowfall to annual runoff, given as a fraction (R). The red lines show the basin area where runoff is dominated by snowmelt. The black lines shows the additional basin areas where runoff is not primarily dominated by snowmelt but water availability is governed by upstream snowmelt. The inset map shows the topographically complex regions of the globe where orographic effects in precipitation occur (Barnett et al., 2005).

The seasonal snowpack in Canada serves as a major component of its regional water resources and acts as a sensitive indicator of climate change (Kang, Shi, Gao, & Déry, 2014). The regular monitoring of the timing and magnitude of streamflow provided by long term data, correlated with climatic variables, provides the means to study climate-related changes in hydrology (Hodgkins, Dudley, & Huntington, 2003).

There are many studies showing the changing condition of snow over the Northern Hemisphere (NH). In the NH, snow cover has retreated poleward at a rate of 5.5 days decade^{-1} resulting in the full snow season (FSS) to decrease at a rate of 0.8 week decade^{-1} (5.3 days decade^{-1}) between the winters of 1972/73 and 2007/08 (Choi, Robinson, & Kang, 2010). Further, it has retracted by 15 to 25 days along eastern Hudson Bay (HB) during the 35-year period (Choi et al., 2010). The spring snow cover extent (SCE) in the NH has significantly diminished over the past century with an accerelating decreasing rate of 7% in March and 11% in April in during 1922 to 2010 (Brown & Robinson, 2011). Similarly, a significant negative trend in snow depth along with SCE is observed in North America over the past 59 years (Dyer & Mote, 2007). Li et al. (2014) showed that there has been a significant decrease in the total winter snow mass in the NH for the period of 1979/80 to 2010/11. Brown & Braaten (1998) reported a significant decline in winter and early spring snow depths with the greatest decreases occurring in February and March over much of Canada including the Hudson Bay drainage basin during the period of 1946 to 1995. There has been a decline in maximum winter snow water equivalent (SWE) in the pan-Arctic region by 0.17 cm decade^{-1} over 1979 to 2009 (Liston & Hiemstra, 2011). Changes in winter snow accumulation or spring snowmelt rates would directly affect the hydrological regime of snowmelt-fed rivers (e.g., permanent streams becoming ephemeral with a decrease in snowpacks) and glacier-fed rivers (e.g., rapid glacier ablation and disappearance) (Buttle et al.,

2012). Further, changes in streamflow into HB may have occurred due to changing snow accumulation and ablation regimes. Therefore, it is important to quantify the contribution of snow to HB river discharge.

Climate change-driven shifts in streamflow timing and magnitude have been reported in North American basins, especially in snow-dominated ones (e.g., Déry et al. 2009; Fritze, Stewart, & Pebesma, 2011; Westmacott & Burn, 1997) and are expected to continue with increased warming. Zhang, Harvey, Hogg, & Yuzyk (2001) reported that the annual and monthly mean streamflow over Canada for the past 30 to 50 years has generally decreased with the greatest changes occurring in August and September. Moreover, they found that the timing of spring peak streamflow has advanced by more than a month (30 days) in many basins of Canada, especially in British Columbia, based on daily streamflow.

Hudson Bay river discharge has experienced changes in its timing and amounts over the past decades. Shiklomanov & Shiklomanov (2003) computed the annual streamflow into HB and Hudson Strait during 1921 to 1965, 1966 to 1976, 1977 to 1987, and 1988 to 1999 and determined it to be 952, 1034, 908, and 878 $km^3 yr^{-1}$, respectively. Similarly, Déry, Stieglitz, McKenna, & Wood (2005) estimated the average annual streamflow input to Hudson, James, and Ungava Bays to be 714 km^3 during 1964 to 2000. Considering HB and James Bay (JB), Déry, Mlynowski, Hernández-Henríquez, & Straneo (2011) estimated a total annual freshwater flux of 760 km^3 into HB from 1964 to 2008.

Changes in river input impact sea ice formation in Hudson Bay that, in turn, affects the climate of north-eastern North America (Saucier et al., 2004). The inflow of fresh water from rivers into the high latitude oceans strengthens the ocean stratification, thereby suppressing deep water

formation. This in turn disrupts or weakens the thermohaline circulation that is responsible for transport of heat and nutrients in the North Atlantic (Ogi, Tachibana, Nishio, & Danchenkov, 2001; Rennermalm, Wood, Weaver, Eby, & Déry, 2007). Further, Etkin (1991) showed that a climate warming of 1°C could advance the sea ice break-up in HB by over two weeks on its eastern side, six to eight days on its southwestern side, and four to seven-days in JB, with freshwater inflows being one of the factors affecting this precise pattern. Earlier spring discharge into HB enhances the advection of ice, creating more open area that grows with time. Therefore, spring river discharge is an important factor impacting the sea ice breakage.

While there are past studies reporting changes in snow and streamflow characteristics in the Hudson Bay region, a study is lacking that relates these hydrological parameters. This research will establish the relationship between changing snow conditions and the river discharge into HB. The study will focus on the spatially-integrated SWE across HB and its contribution to runoff generation in the latter part of the 20th century and early 21st century.

1.2. Goal and Research Questions of the Thesis

The main objective of this research is to assess the changing contribution of snow to runoff generation in the Hudson Bay drainage system during the latter part of the 20th century and the early 21st century.

Research questions:

1. What is the total contribution of snow to HB river discharge?
2. How is the contribution of snow to HB river discharge changing over time?

3. Are there any changes in snow melting onset time that impact the freshwater budget of HB with implications to streamflow timing?

Further, this study will discuss the potential consequences of the changes in the hydrological regime to HB keystone species such as polar bears and ringed seals.

1.3. Structure of the Thesis

The thesis is structured into seven chapters. The first chapter provides an overview of the importance of snow in streamflow generation and the observed shifts in streamflow timing and magnitude driven by climate change as well as a brief literature review on the changing hydroclimatology of HB. In addition, the rationale and goal of the thesis are discussed. Chapter 2 includes background information on the hydrological cycle, water budgets, and impacts of climate change on snow and streamflow in North America and HB. Chapter 3 describes the study area and Chapter 4 discusses the data and tools used and the methods employed for analysis. This chapter includes a detailed explanation and description of trend and statistical analyses performed. Results and discussions follow in Chapters 5 and 6, respectively. Results in Chapter 5 include the validation of data used and temporal and spatial trends of the hydroclimatic parameters used. Furthermore, Chapter 6 provides discussion on the findings and compares and contrasts them with other similar studies. The first part of Chapter 7 presents the concluding summary of the major findings and their discussions. Potential recommendations and future work are discussed in the remainder of Chapter 7.

2. Background

2.1. The Hydrological Cycle

The hydrological cycle describes the distribution and movement of water between the earth and the atmosphere. It involves the continual cycling of water between the hydrosphere, the atmosphere, biosphere, lithosphere and the cryosphere. The cycle is driven mainly by solar heating, leading to the evaporation of water from the oceans and land surfaces. The water vapour is transported by winds, and then condenses to form clouds and precipitation occurs over land and ocean surfaces in the form of rainfall or snowfall. Precipitation may be stored temporarily on land as snow or soil moisture, while the excess runs off and forms streams and rivers, discharging the freshwater into the oceans. This completes the global water cycle (Figure 2).

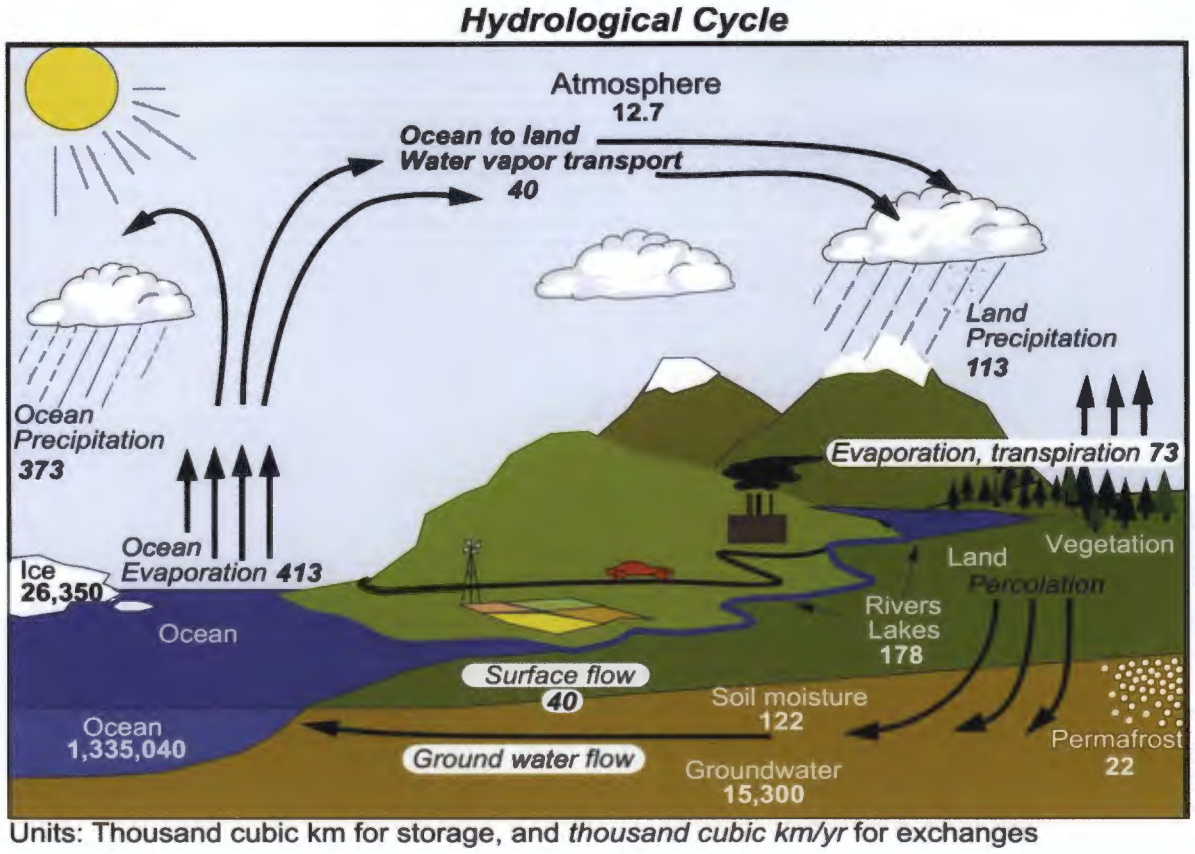

Figure 2. The hydrological cycle (Trenberth, Smith, Qian, Dai, & Fasullo, 2007). The numbers represent the estimates of the main water reservoirs in km^3 (in plain font), and the flow of moisture through the system in $km^3\ yr^{-1}$ (in italicized font).

2.2. Water Budget

A water budget is an accounting framework for the movements and transformations of water in a watershed or region. It describes and quantifies the various components of the hydrologic cycle including precipitation (P), evapotranspiration (ET), runoff (R), and groundwater flow (G_{in}: groundwater inflow, G_{out}: groundwater outflow). These components are related and expressed in a water budget equation as:

$$\Delta S = P + G_{in} - (ET + R + G_{out}) \qquad (2.1)$$

where ΔS is a change in storage.

Precipitation is in the form of rain or snow or a combination of both. When precipitation is in the form of snow, instead of infiltrating the soil immediately or running off into stream channels as surface runoff, water is first stored in the snowpack, often for several months. The winter snowpack melts in the spring thereby contributing to runoff generation. Runoff generated from the melting of snow is the focus of this study. Evapotranspiration is the combination of evaporation and transpiration. Evaporation in snow environments occurs from sublimation and blowing snow, and transpiration by the transfer of water from vegetation to the atmosphere. Runoff is the flux of water at a point or basin scale, expressed in millimetres (mm). In a snow-dominated basin, water from snowmelt represents the dominant portion of the total annual runoff generation. Snowpack is the amount of snow that accumulates on the ground, defined by its local characteristics such as snow depth and SWE. Snow depth (SD) is the thickness or height of snow that remains on the ground at a time of observation, and is typically expressed in centimetres (cm) (Armstrong & Brun, 2008). It changes with processes such as snow transport by wind, settling, metamorphism, sublimation, and melt/refreeze events (DeWalle & Rango, 2008). Therefore, it is not necessarily the most appropriate measure for hydrological studies. SWE is the vertical depth of the water layer that is obtained when the snowpack over a given area is melted (Armstrong & Brun, 2008). It is typically expressed in kg m^{-2} or mm water equivalent. It is measured directly or calculated from measurements of the depth and density of the snowpack (DeWalle & Rango, 2008):

$$\text{SWE} = d(\rho_s / \rho_w) \qquad (2.2)$$

where

SWE = snow water equivalent, m;

d = snowpack depth, m;

ρ_s = snowpack density, kg m^{-3};

ρ_w = density of liquid water, approximately 1×10^3 kg m^{-3}.

The measure of SWE is useful for hydrological applications as it represents the resulting water column when a snowpack melts. In snow dominated basins, runoff from melting of SWE represents a major source of water for streamflow and groundwater recharge. During winter, the snowpack accumulates (i.e. SWE reaches its annual maximum) with very low rates of flow. The flow rate is low due to baseflow recession from prior periods of recharge further reduced by less ground heat conduction to the snowpack base leading to low rates of melt. In spring, as energy supplies for melt increase, the flow rates gradually increase and contribute to runoff, leading to a peak annual flow in late spring or early summer. In high latitude river basins, as much as 80% of the annual streamflow is generated by snowmelt (Déry, Sheffield, & Wood, 2005; McNamara, Kane, & Hinzman, 1998).

SWE_{max} is the maximum SWE value obtained from the available daily SWE data. It is used because it represents the highest value of accumulated snowfall that is metamorphosed by associated atmospheric variables (e.g., temperature, precipitation, wind), landcover type and topography. Snow accumulates during a snow season (usually October to May of a hydrological year) and then melts during spring and summer resulting in runoff (Zhao, Higuchi, Waller, Auld, & Mote, 2013). SWE therefore represents a time-integrated measure of wintertime precipitation, allowing comparison with annual runoff in snow-dominated watersheds. The maximum SWE is an important snow characteristic that helps in operational runoff and river discharge forcast including spring flood (Kokkonen, Koivusalo, Jakeman, & Norton, 2006; Pulliainen, 2006).

Further, this quantity represents the highest value of runoff that is possibly generated from maximum snow accumulated over a hydrological year (Déry et al. 2005).

The hydrological cycle is a closed system and there is a natural balance maintained between the exchange of water within the system. However, human activities can potentially lead to changes in this balance, which will have significant impacts on natural systems. For example, the development of dams and reservoirs for the generation of hydroelectricity could disrupt the natural hydrological cycle. At broad scales, climate warming intensifies the rate of exchange of freshwater between the global atmosphere, land and ocean.

2.3. Climate Change and Snow

It is estimated that the global mean surface air temperatures averaged over land and ocean surfaces have risen by about 0.85 (minimum 0.65 to maximum 1.06) °C over the last 132 years (1880 to 2012) (Hartmann et al., 2013). The rate of warming over the last 60 years (1951 to 2012) is about 0.12 (0.08 to 0.14) °C per decade (Hartmann et al., 2013). In the past 100 years, the mean air temperature rise over the Arctic has almost doubled compared to that of the global mean values (Trenberth et al., 2007). There will be a lesser fraction of the precipitation falling as snow, and an earlier spring snowmelt runoff under the increasingly warmer temperatures, which is expected to occur by the end of the 21st century (Stewart, 2009). With the increasing surface air temperature, the NH snow cover extent (SCE) is decreasing. Brown (2000) estimated the SCE loss of 3.1×10^6 km^2 (100 yr)$^{-1}$ in the NH during 1922 to 1997, associated with significant warming of 1.26°C (100 yr)$^{-1}$.

Furthermore, the satellite records over the period of 1967 to 2012 indicate statistically significant decreases in annual mean SCE in the NH in June (-53%) (Vaughan et al., 2013). Studies by Brown (2000), Brown & Mote (2009), Derksen & Brown (2012), Déry & Brown (2007), Dyer & Mote (2007), and Groisman et al. (2004) show that snow cover has decreased significantly during spring over North America since the latter half of the 20th century. Using satellite and model datasets, Park, Yabuki and Ohata (2012) found that the negative trend of SD over North America between 1948 to 2006 coincides with regional warming patterns. Mote, Hamlet, Clark, & Lettenmaier (2005) reported a declining trend for 1 April SWE across western North America for the period of 1925 to 2000. Brown (2000) found a significant decrease in April SWE in the NH, averaging 4.4% per decade during 1922 to 1997. Liston & Hiemstra (2011) determined a decreasing trend in maximum winter SWE during 1979 to 2009 for most of the pan-Arctic domain.

2.4. Climate Change and Streamflow

Snowmelt runoff in the northern United States and Canada during spring is an important component of its regional hydrology and has a vital influence on water resources (Dyer, 2008). Hodgkins & Dudley (2006) analyzed the changes in the timing and magnitude of winter-spring streamflows that are substantially and regularly augmented by snowmelt runoff in eastern North America over the period of 1913 to 2002. Over the period of 1913 to 1993, Hodgkins & Dudley (2006) found that 64% of stations north of 44°N show significantly earlier flows. The study of the hydrologic consequences of climate change in Rocky Mountain rivers during the 20th century until 2005 reveals declining annual streamflows. Late summer flows have declined at the rate of about 0.2 % yr^{-1} for the rivers draining the eastern slopes of the Rocky Mountains towards

the northern prairies and HB (Rood et al., 2008). Rasouli, Hernández-Henríquez, & Déry (2013) reported a significant reduction of 7.22 km^3 in total streamflow input into Lake Athabasca from 1960 to 2010. Stewart, Cayan, & Dettinger (2005) estimated a change in streamflow timing during 1948 to 2002 in snowmelt-dominated basins across western North America that has shifted by one to four weeks. They considered a broad-scale increase of winter and spring air temperatures by about 1°C to 3 °C over the past 50 years as a primary cause of this change.

2.5. Climate Change in Hudson Bay

Studies have shown that there has been significant warming in the Hudson Bay region in different periods from the early 1990's to 1998; (e.g., Gagnon & Gough, 2002; Gagnon & Gough, 2005a; Gagnon & Gough, 2005b). Hochheim, Lukovich, & Barber (2011) found that the regional spring surface air temperature anomalies surrounding HB have increased from 0.26°C to 0.30°C $decade^{-1}$ over the period 1960 to 2005.

The consequences of warming in the Hudson Bay region are demonstrated by the variability in the timing of sea ice formation and retreat. The mean melt season of Arctic sea ice has increased at a rate of 5.7 ± 0.9 days per decade over the last 34 years (Vaughan et al. 2013). The largest and most significant trends (at the 99% level) of more than 10 days per decade are seen in HB along with other coastal margins and peripheral seas (Vaughan et al. 2013). Gagnon & Gough (2005b) reported statistically significant trends toward earlier breakup in JB, along the southern shore of HB, and in the western half of HB, and toward later freeze-up in the northern and northeastern regions of HB during 1971 to 2003. Further, they found the trends in the annual sea ice cycle of HB coinciding with both the regional air temperature records and the projections from general circulation models.

2.6. Climate Change and Hudson Bay Streamflow

Déry & Wood (2004) revealed the influence of the Arctic Oscillation (AO) on the recent variability in Hudson Bay river discharge with up to 90% of the observed variance being explained. The AO is an atmospheric circulation pattern over northern mid-to-high latitudes (Thompson & Wallace, 1998). Shiklomanov & Shiklomanov (2003) reported that river discharge into HB and Hudson Strait has decreased by 6% from 1966 to1999 as compared to that of 1921 to 1965. Further, a 13% decline in the total annual river discharge into Hudson, James, and Ungava Bays for the period 1964 to 2000 is found by Déry et al. (2005) who analyze the discharge from 42 rivers. Using a linear trend analysis, they observed a decreasing discharge in 36 rivers out of total of 42. Subsequently, Déry et al. (2011) on extending their study period by another eight years found no statistically significant trend in the total annual streamflow into HB. Gagnon & Gough (2002) determined that the eastern HB is experiencing statistically significant warming trends in spring air temperature and three rivers (Grande Baleine, Gods and Kazan) flowing into southern HB show a shift towards an earlier occurrence of spring peak discharge. Further, Déry et al. (2005) discovered that the annual peak discharge rate associated with snowmelt has advanced by eight days between 1964 and 2000 and has diminished by 0.036 km^3 day^{-1} in intensity. A similar trend analysis in unregulated rivers of HB yields an advance of four days in the timing of spring peak discharge rates. The earlier onset of snowmelt is possibly caused by the increasing spring surface air temperature (SAT) in the HB region.

While these studies provide important information on the changing conditions of both snow and streamflow across parts of western North America, there are currently no studies that focus on the spatially integrated SWE across the entire HB and its contribution to runoff generation in the latter half of the 20^{th} century and early 21^{st} century. Therefore, this research covering HB is

motivated by the fact that there exists a gap in quantifying the contribution of snow to the river discharge in terms of its timing and magnitude.

3. Study Area

The study area is the Hudson Bay drainage basin in northeastern Canada. It is the largest drainage basin in Canada where 30% of Canada's water drains. This basin comprises all land areas discharging into HB and JB, covering an area of 3.7×10^6 km^2 or more than a third of Canada's land mass (Déry et al. 2011). The HB system is connected to the Atlantic Ocean by Hudson Strait and the Labrador Sea in the east and to the Arctic Ocean in the north by the Foxe Basin, and Fury and Hecla Straits. The watershed of HB and JB covers a large area from southern Alberta, Saskatchewan, and Manitoba in the west to central Ontario and Québec to the east and the Northwest Territories and Nunavut to the northwest. It also encompasses parts of Montana, North Dakota, South Dakota, and Minnesota in the United States. This vast area drains into the Bay from the glacierized Rocky Mountains in the far west, dry prairies in the continental interior, cool-wet boreal forest in the mid-latitudes, and Arctic tundra in the high latitudes (Déry et al. 2005; Déry et al. 2011).

Twenty important rivers that drain into Hudson Bay and James Bay are listed in Table 1 and presented in Figure 3. These rivers are identified by one of the two bays where they discharge and where their outlet is located in any of the provinces or territories along the HB drainage basin. The mean annual surface air temperature of -2°C prevails in the HB drainage basin and it receives a total annual precipitation of 550 mm yr^{-1}. Snowfall plays an important role in the precipitation of the HB basin, since approximately 155 mm yr^{-1} (30% of its total annual precipitation) falls as snow (Déry & Wood, 2004). The HB drainage basin experiences a a seasonal snowpack cycle each year (Gagnon & Gough, 2005b). The largest streamflow rates into HB are attained during the spring transition period, demonstrating the critical role played by snow in the hydrology of high latitude watersheds (Déry et al. 2005).

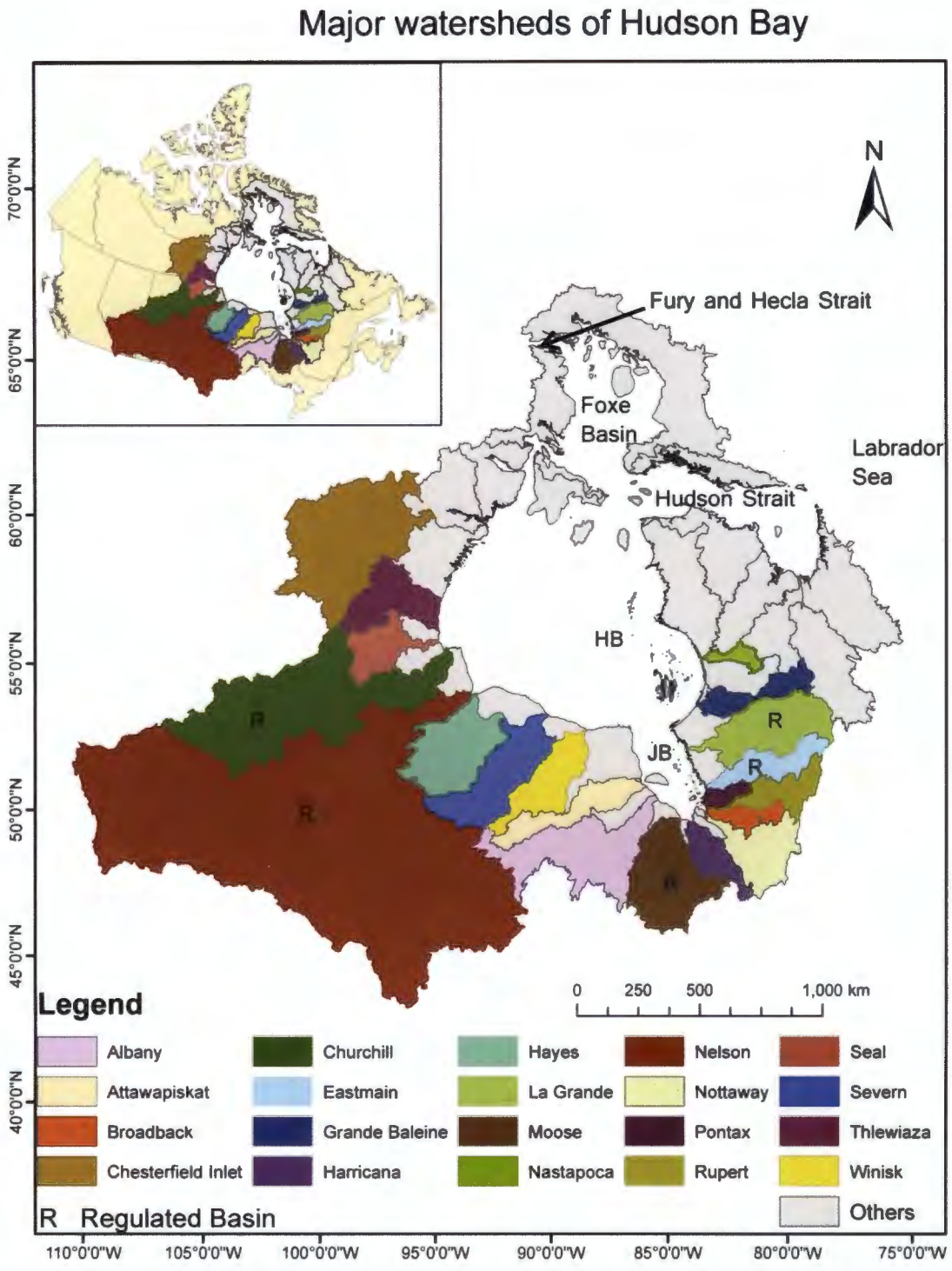

Figure 3. Map of the Hudson Bay Basin showing the 20 rivers with outlets into Hudson Bay or James Bay. The watersheds to the north of Hudson Bay are not gauged and therefore, are not included in the study area. The inset shows the location of Hudson Bay in Canada.

The Hudson Bay basin is home to indigenous and non-indigenous peoples (Figure 4). This area also forms the traditional territories of Inuit and Cree communities living around the perimeter of HB along with 6,000 to 7,000 non-indigenous people (many not permanent residents) (Berkes & Freeman, 1986). There are about 8,530 Cree people living to the west and south of HB in the communities of Chisasibi (4,160), Wemindji (1,315), Eastmain (730), Fort Albany (1,135) and Moosonee (1,190). Further, about 4,460 Inuit people reside along the eastern shores of HB in Arrivat (2,190), Churchill (60), and Kuujjuarapik (495) and Baker Lake (1,715) in the northwestern part of HB (Statistics Canada, 2013). Cities in the Canadian Prairies such as Calgary, Lethbridge, Edmonton, Regina, Saskatoon, Prince Albert, Brandon, and Winnipeg depend on water from the rivers such as the Nelson and Churchill for hydropower, agriculture, industries, recreation and other activities. Many rivers flowing into HB are a major source of water for hydroelectric generation in central and eastern Canada (e.g., in Manitoba, Ontario and Québec; Manitoba Wildlands, 2005; Rosenberg et al., 2005).

The ecozone of Hudson Bay supports a large diversity of plants and animals. HB provides habitat for different marine and terrestrial mammals, fish, and migratory birds. Ringed seals and the polar bears are the keystone species of the region (Ferguson, Stirling, & Mcloughlin, 2005; Smith, 1975; Stirling, 2005; Regehr et al., 2007). An areal survey in western HB in 2011 recorded a total of 711 polar bears sightings along the coastline (Atkinson, Garshelis, Stapleton, & Hedman, 2012). In addition, the Department of Fisheries and Oceans (DFO) (DFO, 2011) estimated the abundance of ringed seals at 62,157±5,344 in June 2010 in western HB. However, there are studies showing declining populations of these species during 1990 to 2010 (DFO 2009; DFO 2011; Lunn, Stirling, & Nowicki 1997; Regehr, Lunn, Amstrup, & Stirling, 2007). Further, there are some cases of seals and humans being infected by parasites such as *toxoplasma*

gondii reported during period of 1999 to 2008 associated with changes in snowmelt runoff in the HB basin (Simon, Bigras-Poulin, Rousseau, & Ogden, 2013; Simon, Rousseau, Savary, Bigras-Poulin, & Ogden, 2013).

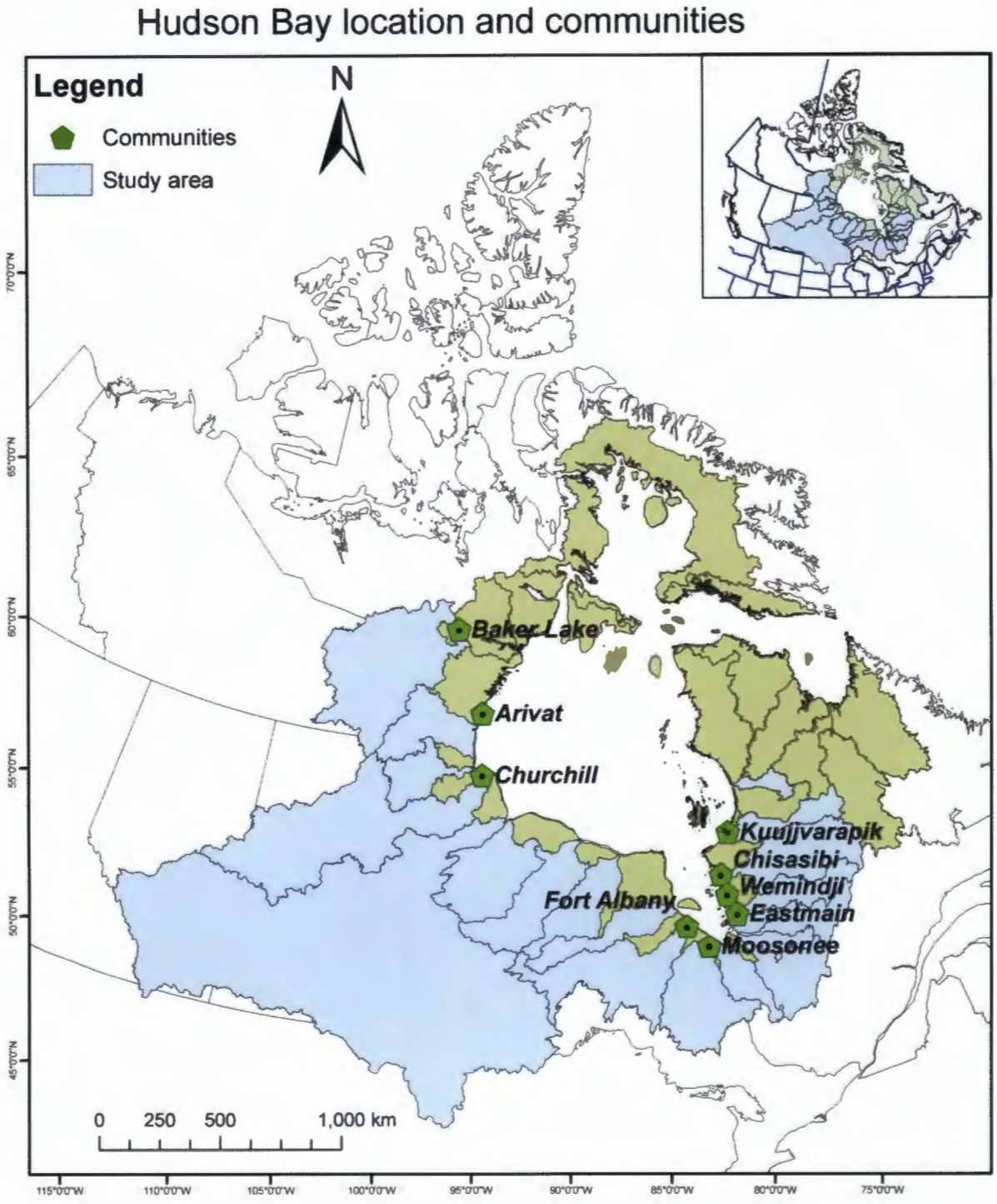

Figure 4. The largest communities surrounding the Hudson Bay coastline.

Table 1. Alphabetical list of 20 rivers that discharge into Hudson Bay (HB) and James Bay (JB), and their outlet, province or territory (ON refers to Ontario, QC: Quebec, NU: Nunavut, and MB: Manitoba), geographical coordinates of the recording hydrometric gauge nearest to the mouth, contributing area that is gauged, and their condition. NAT indicates the river is naturally flowing and REG indicates the river is regulated. Note that some of these rivers include small downstream tributaries (see Appendix 3).

River	Outlet	Province/ Territory	Latitude (°N)	Longitude (°W)	Area (km^2)	Regulation Type
Albany	JB	ON	51.33	83.84	118,000	NAT
Attawapiskat	JB	ON	53.09	85.01	36,000	NAT
Broadback	JB	QC	51.18	77.43	17,100	NAT
Chesterfield Inlet	HB	NU	64.31	101.21	224,000	NAT
Churchill	HB	MB	58.12	94.62	290,880	REG
Eastmain	JB	QC	52.24	78.07	44,300	REG
Grande Baleine	HB	QC	55.29	77.59	43,200	NAT
Harricana	JB	QC	49.95	78.72	21,200	NAT
Hayes	HB	MB	56.43	92.79	103,000	NAT
La Grande	JB	QC	53.72	78.57	96,600	REG
Moose	JB	ON	50.81	81.29	98,530	REG
Nastapoca (Loups Marins)	HB	QC	56.86	76.21	12,500	NAT
Nelson	HB	MB	56.37	94.63	1,075,520	REG
Nottaway	JB	QC	50.13	77.42	57,500	NAT
Pontax	JB	QC	51.53	78.09	6,090	NAT
Rupert	JB	QC	51.44	76.86	40,900	REG
Seal	HB	MB	58.89	96.27	48,200	NAT
Severn	HB	ON	55.37	88.32	94,300	NAT
Thlewiaza	HB	NU	60.78	98.77	27,000	NAT
Winisk	HB	ON	54.52	87.23	54,710	NAT
Total					**2,509,530**	

Among the 20 rivers in this study, the two largest rivers by volumetric flows are the Nelson and La Grande Rivière (Déry et al., 2011). There have been major disturbances in many rivers draining into HB since the 1960s due to the construction of dams, reservoirs and diversions of small rivers into larger ones for hydropower development. The six major rivers that drain into

HB impacted by dams, diversions (i.e. intra- and inter-basin), and/or reservoirs are listed in Table 2.

Table 2. List of rivers that are affected by major dams, diversions (DIV), and/or reservoirs (RES) as well as the approximate year when major human impacts began (Déry et al. (2005); Hernández-Henríquez, Mlynowski, & Déry, (2010)).

River	Human Impact	Year
Churchill	DIV	1976/77
Eastmain	DIV	1980
La Grande	dam, RES	1980
Moose	dam	1911
Nelson	dam	1926
Rupert	DIV	2009

Hydropower production from the main stem of the Nelson River started in 1961 (Rosenberg et al. 2005); however, hydropower plants have operated since 1926 on the Winnipeg River, a tributary of the Nelson River (Manitoba Hydro, 2015). In 1976, 75% of the Churchill River's flow was diverted into the lower Nelson River to augment flows for long-term hydropower development in that system (Newbury, McCullough, & Hecky, 1984), making the average discharge of the Nelson River 78.2 km^3. Therefore, in this study, the Nelson and Churchill River Basins are considered as one large basin known as the Nelson-Churchill. The Churchill and Nelson are Manitoba's largest rivers. They support seven hydroelectric stations and more additions are proposed for the future (Manitoba Wildlands, 2005). Similarly, in the Moose River Basin, the river was fragmented by more than 40 dams and water-control structures. The construction of the oldest structures extends back to 1911 to 1932 with most of remaining dams constructed in the 1960s (Rosenberg et al. 2005). In 1980, the northward diversion of the Eastmain and Opinaca Rivers to La Grande Rivière reduced 90% of the downstream flow from the Eastmain River (Hernández-Henríquez, Mlynowski, & Déry, 2010). Further, a portion of the

upper Caniapiscau River since 1984, and a portion of the Rupert River since 2009 have been diverted into La Grande Rivière by Hydro-Québec (Hernández-Henríquez, Mlynowski, & Déry, 2010). However, the Rupert River is still examined as a stand-alone basin in the present study but only until 2006. Due to the diversion of the Eastmain River into La Grande Rivière throughout the entire study period, they are considered as one large system termed La Grande-Eastmain.

3.1. Hudson Bay Drainage Basin

The Hudson Bay drainage basin is a large, snow-dominated drainage basin and the world's largest northern inland sea. HB and Hudson Strait contribute about 946 $km^3 yr^{-1}$ of freshwater (during 1921 to 1999) or $1/5^{th}$ of the total annual river discharge to the Arctic Ocean (Shiklomanov & Shiklomanov, 2003). The HB bridges the Arctic and temperate domains of central Canada and therefore, represents an important site for cryospheric change (Macdonald & Kuzyk, 2011). Furthermore, the export of freshwater from HB to the Labrador Sea by ocean currents contributes to its salinity variability that in turn influences high latitude oceanographic, atmospheric, cryospheric, and biologic processes (LeBlond, Lazier, & Weaver, 1996).

There may be significant impacts of climate change on the hydrologic regime of HB with implications for native species, hydropower generation and local communities, and the overall economy of northeastern Canada. For example, with an increasing air temperature, the population of native species such as seal and polar bear is decreasing in the HB region (Regehr et al., 2007; Norris, Rosentrater, & Eid, 2002; Peacock, Derocher, Lunn, & Obbard, 2010; Ferguson et al., 2005; Dyck et al., 2007). Further, the changing climate affects the present and future capacity of hydropower generation and operations of hydroelectric developments over the high latitude region of Canada (Prowse et al., 2009; Minville, Brissette, Krau, & Leconte, 2009).

Climate change has implications for the well being and traditional life styles of the indigeneous population in the HB region. It has affected animal behaviour, impacted the traditional harvesting activities of Cree communities and the winter-road system causing more ice roads (Tam, Gough, Edwards, & Tsuji, 2013). In addition, other sectors of the economy, such as oil and gas, mining, infrastructure and transportation, face challenges due to climate change as they are developed and engineered around the cryospheric components of northern Canada (Prowse et al., 2009).

4. Data Collection and Methods

This chapter describes the data and methods used for the study. The first part looks at different sources of data considered and the description of the data used for analysis. The second part explains the methods used for long-term trend analyses and their statistical significance.

4.1. Data Collection

The main data used in this study are the SWE and streamflow data that are discussed below.

4.1.1 SWE Data

For this research, the daily GlobSnow SWE (version 2.0) dataset developed by the European Space Agency (ESA) is used (available at http://www.globsnow.info/swe/archive_v2.0/). The SWE data extend from 1979 to 2013 for the NH land surface areas, except for mountainous regions, glaciers and Greenland and has a spatial resolution of 25 km × 25 km. Data for the HB domain are then clipped out of the NH SWE. The GlobSnow SWE data are selected for this study because they are available for a longer period of time at a daily time scale with a reasonable spatial resolution to calculate the SWE at the basin level.

The GlobSnow SWE is produced by using a combination of satellite microwave radiometer and ground-based weather station data. It utilizes space-borne passive radiometer data from different sensors for different time periods, including the Scanning Multichannel Microwave Radiometer (SMMR) for 1979 to 1987, the Special Sensor Microwave/Imager (SSM/I) for 1987 to 2009 and the Special Sensor Microwave Imager/Sounder (SSMIS) for 2010 to 2013. The weather station synoptic data for GlobSnow are provided by the European Centre for Medium-Range Weather Forecasts (ECMWF). These forecasts give the measured snow depth at station locations across the NH (Luojus et al., 2013). Inclusion of a large number of in situ measurements of snow depth in the GlobSnow's inversion algorithm has improved its accuracy (Luojus et al., 2010).

The sensors provide brightness temperature data at K- and Ka-bands (19 GHz and 37 GHz, respectively) and are all acquired from the National Snow and Ice Data Center (NSIDC) in Equal-Area Scalable Earth (EASE)-Grid projection with a nominal spatial resolution of 25 km (Luojus et al., 2013). To derive the SWE data from remote sensing and ground based data, first wet/melting snow areas are masked out using an empirical relationship between brightness temperatures and snow properties. The sensors measure the brightness temperature that depends on the characteristics of a single-layer snowpack (depth, bulk density and grain size) and the forest canopy. The snow depth is obtained from brightness temperatures for grid cells assembled with weather station data using an emission model. The model uses the snow grain size as a scalable input parameter that is chosen to minimize the difference between observed and computed snow depth. The set of grain sizes obtained together with the snow depth is distributed by a kriging interpolation, that is further used in the emission model inversion to obtain the snow depth distribution. The snow depth is then converted into SWE using the snow density values obtained from Sturm et al. (2010).

The SWE dataset has been validated using independent SWE reference data from Russia, the former Soviet Union, Finland and Canada. It was found that the root mean square error (RMSE) was below 40 mm for cases when SWE was less than 150 mm, indicating an overall good performance for SWE estimation at the hemispheric scale (Takala et al. 2011). Details on this methodology for SWE extraction and validation can be obtained from Takala et al. (2011). Further, Takala et al. (2011) performed validation of GlobSnow SWE for Canada by comparing its seven-days moving average SWE with reference ground SWE measurements for the period of 2005/06-2007/08. The reference ground measurements of SWE were obtained from various Canadian landcover regions such as from an intensive ground survey in the Northwest

Territories, snow surveys by SnowSTAR, Environment Canada and Boreal Ecosystem Research and Monitoring Sites (BERMS). Further, a study by Liu, Li, Huang, & Tian (2014) has validated the GlobSnow SWE using ground station snow depth measurements from the Global Historical Climatology Network-Daily (GHCN-DAILY) that is obtained from 7388 meteorological stations over the NH. They found the correlation coefficient for GlobSnow SWE >0.5 for the NH during 1979 to 2010 when SWE is above 30 mm and below 200 mm.

4.1.2 Streamflow Data

The daily observed discharges for the 20 rivers in this study are obtained from the Water Survey of Canada (available at http://wateroffice.ec.gc.ca/search/search_e.html?sType=h2oArc) for 1979 to 2013 and le Centre d'Expertise Hydrique du Québec for Québec for 2000 to 2013. The streamflow data from 1979 to 2013 for La Grande-Eastmain Rivers are provided by Hydro-Québec. For the Rupert River, streamflow data are available until 2006 as afterward the hydrometric gauge was discontinued, and as the flows were starting to be diverted towards La Grande Rivière. However, since the Rupert River was diverted only in 2009 and due to availability of its streamflow data until 2006, it is included in a list of unregulated rivers for analysis in this study. Further, runoff from a portion (about 36,900 km^2) of the Caniapiscau River was diverted into La Grande Rivière starting in 1984 changing the contributing area. The streamflow data for the Harricana River are available only until 2004 because there are no other data after this date for its principal tributary, the Turgeon River. The data quality control and assessment are described below in Section 4.1.3. The mean annual discharge is divided by the overall gauged area to calculate a mean water year runoff rate that is expressed in mm. A detailed error analysis for the streamflow data is not done in this study. However, it is assumed

to be similar to the studies by Lammers, Shiklomanov, Vörösmarty, Fekete, & Peterson (2001) and Shiklomanov et al. (2006). Lammers et al. (2001) reported a typical error range of ±2-5% for non-ice conditions in river regions without a flood plain and ±5-12% with a flood plain for river discharge measurement. Further, for the six largest Eurasian pan-Arctic rivers, Shiklomanov et al. (2006) estimated the error range to be 1.5-3.5% in total annual discharge over the period from 1950 to 2000.

The SWE and streamflow data are arranged by hydrological years and analyzed. A hydrological/water year is defined here to begin on 1 October and end on 30 September of the following calendar year. This is used because snow accumulates in autumn and winter and does not melt and drain until the following spring or summer. Therefore, using a hydrological year helps to obtain a better correspondence between runoff and snowfall in a period of one year.

4.1.3 Data Quality Assessment and Control

For the GlobSnow SWE data, missing gaps are inspected at each grid cell within the study domain. The missing gaps identified as NA are removed and then the dataset is used for analysis. There are some missing daily values of GlobSnow SWE data in each year, and the sequence of missing data is not regular. Further, information on why they are missing is not available; therefore, they are assumed to be missing because of technical issues. This could be considered as a further limitation of the SWE data availability. Such missing daily values of GlobSnow SWE data were not in-filled because daily SWE_{max} is used for this study. Obtaining SWE_{max} from daily SWE and interpolating or filling with mean values for missing values would result in a lesser SWE value that cannot be considered as SWE_{max}. Therefore, the original GlobSnow SWE data available are used in this study.

Missing gaps in incomplete streamflow series are in-filled following Déry et al. (2011) in a two-step process. In the first step, missing data of the downstream gauge of a river are in-filled using the streamflow data from the nearest upstream station and the discharge for the missing area between the two gauges that is contributing to streamflow is adjusted based on the difference in contributing area. Secondly, when the additional data from an upstream gauge are missing, the data gaps are in-filled with mean daily discharge values over the period of record at each of the gauges. A 12-year data gap in the Severn River of Ontario that exists in latter part of study period (from 1996 to 2007) is filled using this method.

4.2 Methods

4.2.1 Tools

Statistical analysis and calculations in this study are performed using R and ArcGIS. R is a freely available computer programming and software environment that is widely used for statistical computing and graphics (R Development Core Team, 2011; Zuur, Ieno, & Meesters, 2009). The Environmental Systems Research Institute's (ESRI's) ArcGIS 10.1 is used for watershed delineation and generating maps (ESRI, 2011).

4.2.2 General Statistics

Mean and Standard Deviation

Mean ($\bar{x}$) and standard deviation (σ) of the annual runoff and SWE_{max} in each of the HB rivers is calculated from (von Storch & Zwiers, 1999):

$$\bar{x} = \frac{1}{n}\sum_{i=1}^{n} x_i \qquad (4.1)$$

$$\sigma = \sqrt{\frac{\sum_{i=1}^{n}(x_i - \bar{x})^2}{(n-1)}} \qquad (4.2)$$

where $x_i, i = 1, \ldots\ldots\ldots, n$ is the series of the data.

Coefficient of Variation (CV)

The extent in variability in relation to mean annual runoff and SWE_{max} in each of the HB rivers is calculated using the coefficient of variation (C_v; Abdi, 2010):

$$C_V = \frac{s}{\bar{x}} \qquad (4.3)$$

where s is standard deviation, and $\bar{x}$ is the mean.

Percent Change

Percent change in annual runoff and SWE_{max} in each of the HB rivers is calculated by multiplying the linear trend of annual runoff and SWE_{max} with years of study and dividing it with the value in a base year. It is then changed to a percentage value.

Let m be the linear trend of annual runoff, n be the number of years of study and R_1 be the annual runoff value of the initial year of a time series, then the percent change *(% Change)* is given by:

$$\%\ Change = \frac{m \times n}{R_1} \times 100\% \qquad (4.4)$$

For the calculation of percent change in annual SWE_{max}, R_1 in Equation (4.4) is replaced by $SWE_{max(1)}$ that represents the annual SWE_{max} value of the initial year of a time series, m represents the linear trend of an annual SWE_{max}, and n is the number of years of study.

Spatial Averaging

Spatial average of annual runoff and SWE_{max} in eastern and western HB, regulated and unregulated HB and overall HB is calculated by multiplying the annual runoff or SWE_{max} with the area of that basin and dividing the sum of it by the total area of the basins.

Let R_1, R_2, R_3, ..., R_n be the annual runoff of each river, and A_1, A_2, A_3, ..., A_n be the area of each river basin, where n is the number of the river, then the spatial average (S.A.) is given by:

$$S.A. = \frac{R_1 \times A_1 + R_2 \times A_2 + R_3 \times A_3 + \ldots + R_n \times A_n}{A_1 + A_2 + A_3 + \ldots + A_n} \qquad (4.5)$$

For the spatial average of SWE_{max}, R_1, R_2, R_3, ..., R_n in Equation (4.5) are replaced by $SWE_{max(1)}$, $SWE_{max(2)}$, $SWE_{max(3)}$, ..., $SWE_{max(n)}$, where $1, 2, 3, \ldots, n$ represent the annual SWE_{max} of each river basin. The spatial average of runoff or SWE_{max} for subsets of HB may be greater or less than the value for overall HB since the spatial average depends upon the area considered for the analysis.

4.2.3 Validation

The GlobSnow SWE data are validated using the monthly estimated SWE data obtained from the Canadian Meteorological Centre (CMC). At CMC, monthly average SWE (mm) is estimated from monthly average snow depth multiplied by mean monthly snow density values, derived from Canadian snow course observations corresponding to snow climate classes given by Sturm, Holmgren, & Liston (1995). The snow depth data used are analyzed on a 24 km × 24 km grid from 1998 to the present (Brown & Brasnett, 2013). The monthly SWE estimates from CMC are driven by precipitation from the Global Environmental Multiscale (GEM) forecast model in areas without snow depth observations (most of the study domain). The SWE data are available at http://nsidc.org/data/nsidc-0447.html. The monthly average SWE are available only from October to June of each year because of the lack of observed snow density information during the remaining time period. Further, when the monthly SWE is zero, those data are not included in the statistics. The monthly GlobSnow SWE is compared with observed monthly SWE of the available hydrological years from 1999 to 2011.

4.2.4 Evaluation Statistics

Correlation

The correlation between the GlobSnow and observed SWE is calculated using the Pearson's product moment correlation coefficient (Rodgers & Nicewander, 1988). It is given by:

$$r = \frac{\sum_{i=1}^{n}(X_i - \bar{X})(Y_i - \bar{Y})}{\sqrt{\sum_{i=1}^{n}(X_i - \bar{X})^2}\sqrt{\sum_{i=1}^{n}(Y_i - \bar{Y})^2}} \quad (4.6)$$

where, r is the correlation, X is the GlobSnow SWE, $\bar{X}$ is mean GlobSnow SWE, Y is the observed SWE and $\bar{Y}$ is its mean. The r is considered statistically significant if $p<0.05$ in this work.

Root Mean Square Error (RMSE)

The RMSE is the square root of the average squared difference between the GlobSnow and CMC SWE data. It is used to measure the difference between values predicted by the two datasets. It is calculated as (Wilks, 2011):

$$RMSE = \sqrt{\frac{1}{n}\sum_{i=1}^{n}\left(x_{obs,i} - x_{model,i}\right)^2} \quad (4.7)$$

where x_{obs} are observed values and x_{model} are gridded values at time i.

Nash-Sutcliffe efficiency (NSE) coefficient

The accuracy of the GlobSnow SWE is also quantified using the Nash-Sutcliffe efficiency (NSE) coefficient (Nash & Sutcliffe, 1970). The NSE score shows how accurately the GlobSnow SWE data represent the CMC SWE data in HB. NSE coefficients range from -∞ to 1; the closer the NSE is to 1, the more accurate the model is. It is calculated by:

$$\text{NSE} = 1 - \frac{\sum_{i=1}^{n}(X_{obs,i} - X_{model,i})^2}{\sum_{i=1}^{n}(X_{obs,i} - \bar{X}_{obs,i})^2} \qquad (4.8)$$

where X_{obs} is the observed data and X_{model} is the modelled data, and $\bar{X}_{obs}$ is the mean of the observed data.

4.2.5 Analysis

4.2.5.1. Contribution of Snow to Runoff Generation

At first, hydrological year maximum daily SWE (SWE_{max}, mm) for each grid point falling within a given watershed is tracked. If SWE_{max} for any of the grid points is not available, then it is filled as NA. Then, available SWE_{max} values are spatially averaged across a watershed (see Figure 5) and divided by the hydrological year runoff (R, mm). This ratio is termed as R_{SR}. To quantify the contribution of snow to HB streamflow generation, R_{SR} each water year is obtained from:

$$R_{SR} = \frac{\overline{SWE}_{max}}{R} \qquad (4.9)$$

where, $\overline{SWE}_{max}$ is hydrological year spatially averaged maximum SWE and R is the runoff (mm yr^{-1}) (Déry, Sheffield, & Wood, 2005). The spatially averged SWE_{max} gives the potential amount of water stored during autumn and winter in the snowpack distributed throughout a basin that would yield runoff upon melting. The runoff is first obtained by dividing the simulated

streamflow by the corresponding watershed area. Then the daily runoff over a given hydrological year is temporally integrated to obtain total annual runoff at a selected basin.

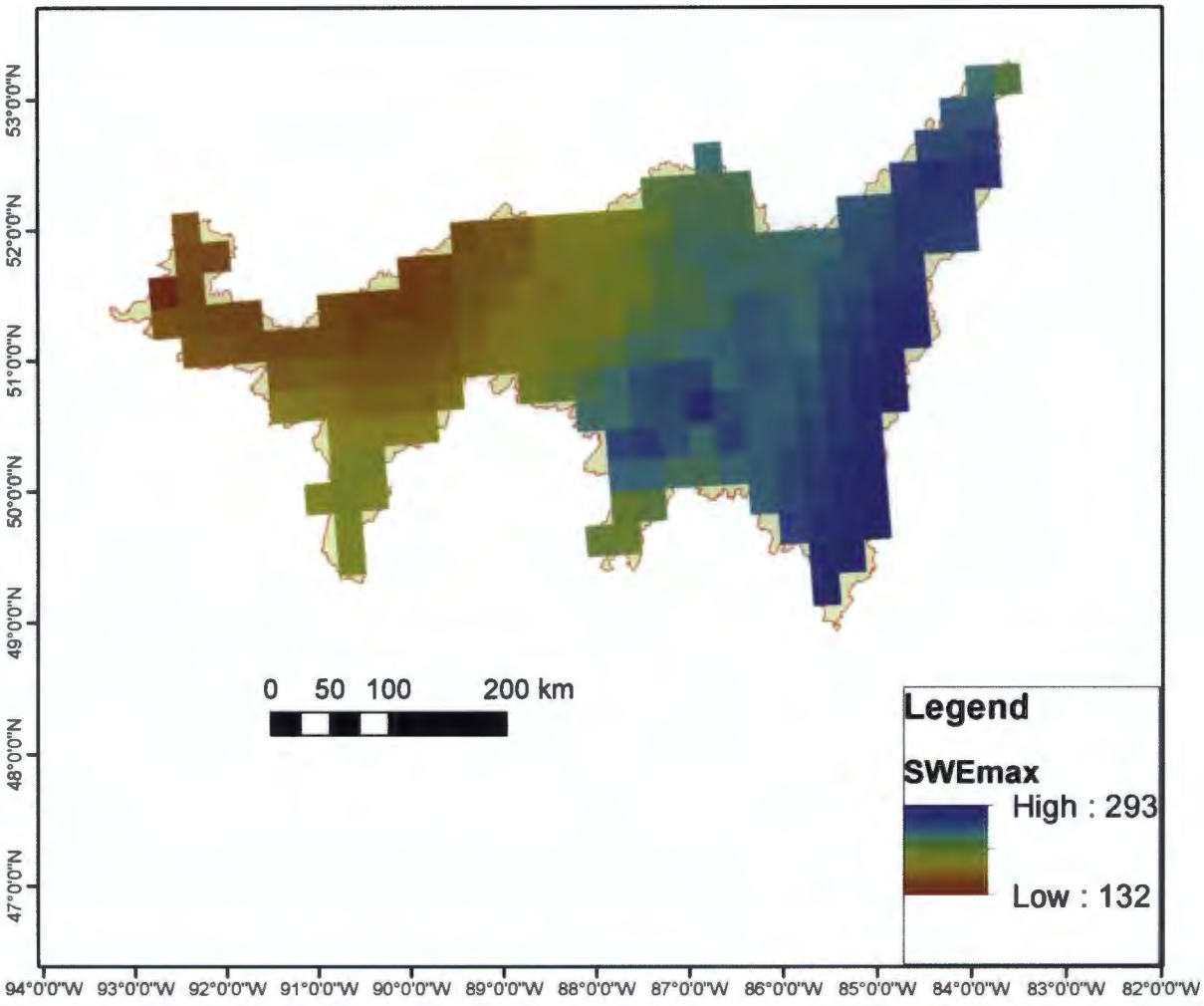

Figure 5. Map of the 2007 SWE_{max} (mm) for the Albany watershed showing all points within it and their SWE_{max} values.

4.2.5.2. Trend Analysis

Temporal trends of river discharge and other hydrometeorological variables are evaluated using the Mann-Kendall non-parametric test (Kendall, 1970; Mann, 1945). This test is found to be a robust tool for trend analysis in similar hydroclimatic studies as it does not rely on the magnitude of data or assumptions on their distribution (e.g., Déry & Wood, 2004; Déry et al. 2005; Déry & Brown, 2007; Kang et al. 2014; Shi, Déry, Groisman, & Lettenmaier, 2013). Trend magnitude is assessed using the Kendall-Theil Robust Line (Déry et al. 2005; Sen, 1968). It develops a linear equation from a time series of n elements such as

$$y = mt + b \qquad (4.10)$$

where t is time in years and y denotes river discharge. To determine the slope m of Equation (4.9), the slopes m_k for each tied group of river discharge data are computed as

$$m_k = \frac{(y_j - y_i)}{(t_j - t_i)} \qquad (4.11)$$

where k=1, 2, …, $n(n\text{-}1)/2$; i= 1, 2, …, n-1; and j= 2,3,…, n. where n is the total number of values. The median slope of all elements m_k is then considered as the slope of Equation (4.10). The coefficient b is obtained by substituting the median time and river discharge values in Equation (4.10) and solving for b. This provides the Kendall-Theil Robust Line for each time series of river discharge as well as the magnitude of this trend (m). The significance of the test is observed at a 95% confidence interval.

4.2.5.3. Change in Melt Onset Date Impacting Streamflow Timing

The change in melt onset date is assessed following the methodology proposed by Déry et al. (2009). It is studied here in unregulated rivers to see the change in streamflow timing of naturally flowing rivers. For each hydrological year, the 365 daily runoff values are segregated and then the monotonic trends for each of the daily time series is calculated from the slope of the Kendall-Theil Robust Line (see equations 4.10 and 4.11). Using the trend magnitude, an assessment of the date of change in runoff timing is generated. Further, a moving average curve is added in the time series plots of the daily runoff trend of each river. Here, a seven-day moving average of the daily runoff trend is calculated to smooth out the daily fluctuations. It is calculated by taking the arithmetic mean of seven consecutive runoff trend values of a time series. The moving average curve is calculated as given in Equation 4.12 (McCuen, 2003):

$$x_i' = \frac{1}{7}\sum_{j=1}^{7} x_{i+j-3} \; for \; i = 4, \ldots\ldots, n-3 \qquad (4.12)$$

where x_i is the time series of the runoff. The seven-day moving average is a new series obtained by taking the arithmetic mean of seven consecutive values of x_i.

Further, to study the change in the annual hydrological condition of rivers, the study period is divided into two equal periods of 17 hydrological years from 1980 to 1996 and 1997 to 2013. In the case of the Rupert and Hayes Rivers the initial periods are 1980 to 1992 and 1980 to 1991 and latter periods are 1993 to 2006 and 1992 to 2004 respectively as the streamflow data for this river end in 2006 and 2004 respectively. Then for each period the daily runoff values are averaged and an annual hydrograph is plotted. The annual hydrographs of two periods are then compared to study the changing hydrological condition.

5. Results

The results of the analysis of runoff and SWE data over the Hudson Bay watersheds are presented in this chapter. The trends and statistical analysis of SWE data are shown first, followed by the analysis of runoff. The basic statistical analyses are presented in tabular format to provide general information of the hydrologic conditions of HB watersheds. The analyses are done for individual rivers and spatial means of the hydrologic parameters for all rivers are taken to represent an analysis for the entire HB. Further, the analyses are presented for the eastern and western sections of HB as well as for regulated and unregulated rivers of the HB drainage basin. The eastern part comprises nine rivers (Broadback, Grande Baleine, Harricana, La Grande-Eastmain, Nastapoca, Nottaway, Pontax and Rupert) and the western part comprises 11 rivers (Albany, Attawapiskat, Chesterfield Inlet, Hayes, Moose, Nelson-Churchill, Seal, Severn, Thlewiaza, and Winisk). There are five regulated rivers and 15 unregulated rivers (see Table 1 and 2 and Figure 3) in the HB watersheds used in this study.

The results of the validation of selected SWE data with an independent dataset are presented. This is performed using Pearson's correlation coefficient (r) and corresponding p-values, RMSEs, and NSE coefficients to verify the reliability of the data. Further, the contribution of snow to runoff generation and their trends in HB watersheds are analyzed and presented. The last section of this chapter includes the analysis of the daily runoff trends for each of the unregulated rivers to see change in the melt onset date impacting streamflow timing in HB watersheds.

5.1. Validation of GlobSnow SWE Data

The CMC monthly SWE data from 1998 to 2011 for the Albany, Broadback, Chesterfield Inlet and Grande Baleine watersheds are compared with the monthly average GlobSnow SWE data. The four watersheds are selected to validate at least 20% of the selected rivers in the study area. They cover different portions of the HB drainage and different snow and vegetation regimes.

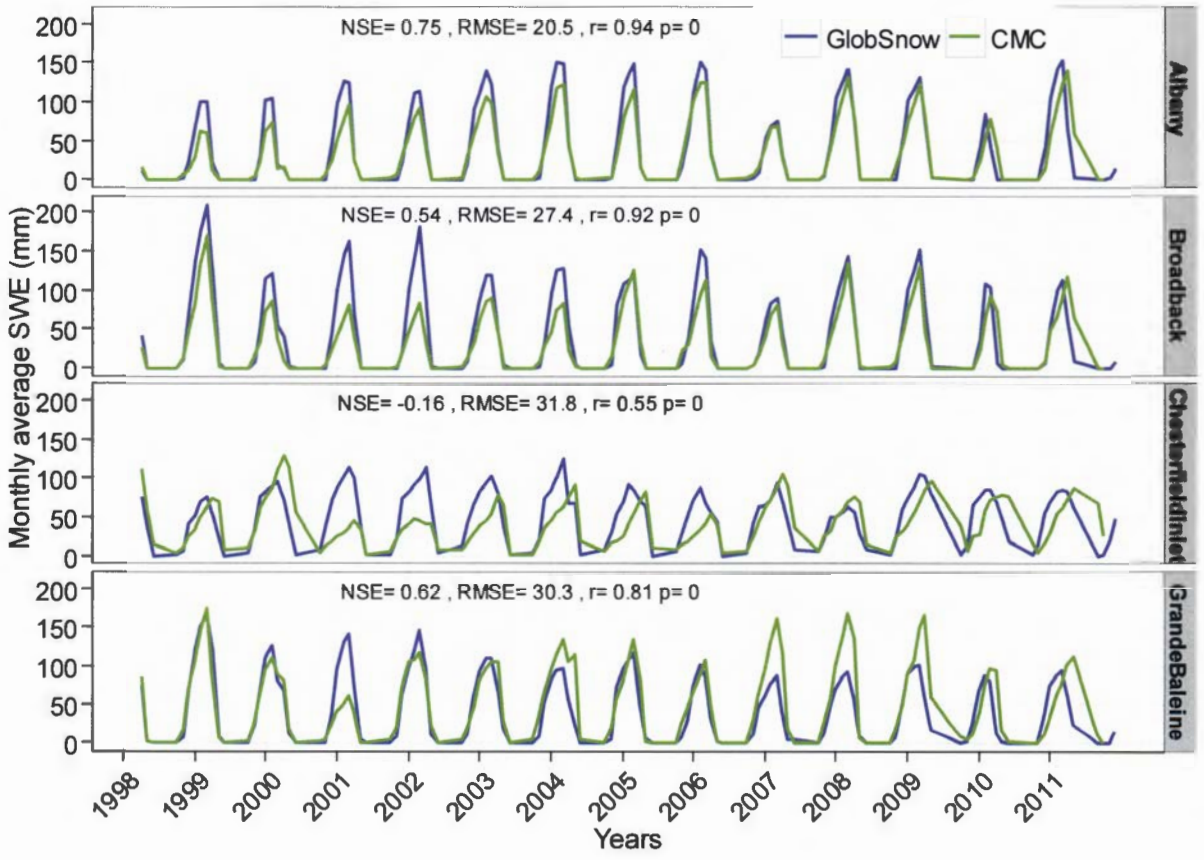

Figure 6. Monthly average SWE (CMC and Globsnow) with NSE, RMSE, *r* and *p*-value, 1998 to 2011.

Figure 6 shows the comparison of GlobSnow and CMC monthly average SWE data for the four watersheds with their NSE, RMSE, *r* and *p*-values. The GlobSnow SWE data correlate well with

CMC SWE data in all watersheds. While the NSE for monthly averaged SWE is slightly negative for the Chesterfield Inlet watershed (-0.16), it is >0.5 for all other watersheds. The correlations are greater than 0.80 for these three watersheds and is 0.55 for Chesterfield Inlet, all being statistically significant. The RMSEs for monthly averaged SWE shows a difference of up to 31.8 mm for the Chesterfield Inlet watershed. This is comparable to the overall RMSE of about 40 mm estimated for the GlobSnow SWE over the Canadian land coverage and 47 mm specific to the tundra region (Takala et al. 2011). Further, the difference observed in the Chesterfield Inlet could be due to lack of in situ data in the high latitude that leads to degradation in CMC SWE quality. Overall, GlobSnow overestimates SWE relative to CMC for most years.

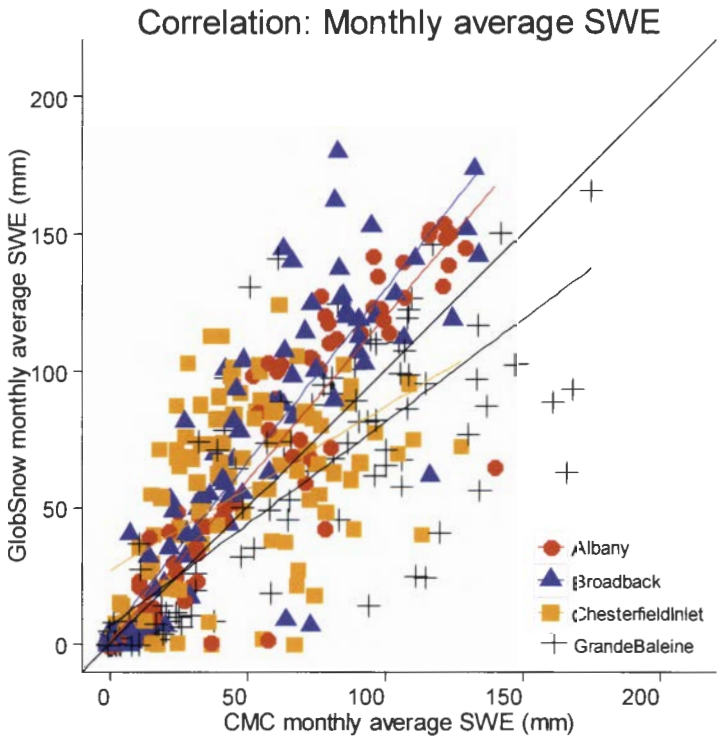

Figure 7. Comparison of monthly average SWE from CMC and Globsnow for four Hudson Bay watersheds for the period 1998 to 2011. The solid diagonal line is the 1:1 line.

The correlation between GlobSnow and CMC monthly average SWE for the Albany, Broadback, Chesterfield Inlet and Grande Baleine watersheds is shown in Figure 7. There is a strong correlation for the Albany, Broadback and Grande Baleine watersheds, but CMC SWE overestimates the GlobSnow values for the Chesterfield Inlet watershed. This might be caused by overestimation of snow depth in that particular basin (Brown & Brasnett, 2013).

5.2. Characteristics and Trends of SWE_{max} in Hudson Bay Watersheds

The mean annual, standard deviation and coefficient of variation in annual SWE_{max} for the HB 20 watersheds are presented in Table 3. The monotonic trends in annual SWE_{max} for each watershed with slopes and percentage change during the period from 1980 to 2013 are also included in the table. The analysis shows that the Rupert watershed has the highest mean SWE_{max} (197.6 mm) from 1980 to 2013. Other watersheds that have higher SWE_{max} over the study period are the Harricana, Broadback, La Grande-Eastmain and Moose watersheds that lie in the southeastern part of the study area.

Table 3. The 1980 to 2013 annual mean, standard deviation (SD), coefficient of variation (CV), trend, and percent change in SWE_{max} for the 20 watersheds of interest.

Watershed	Annual SWE_{max} statistics				
	Mean (mm)	SD (mm)	CV	Linear Trend (mm yr^{-1})	Percent Change (%)
Albany	159.9	28.1	0.17	-0.2	-4.1
Attawapiskat	152.4	27.8	0.18	-1.1**	-20.8
Broadback	182.6	34.3	0.18	-1.1**	-31.1
Chesterfield Inlet	134.5	21.7	0.16	-1.0**	-23.3
Grande Baleine	159.5	26.5	0.16	-0.9	-20.8
Harricana	190.0	27.8	0.14	-0.4**	-8.0
Hayes	142.9	24.6	0.17	-1.2**	-26.8
La Grande-Eastmain	180.6	30.2	0.16	-1.4	-30.9
Moose	179.2	37.0	0.20	-0.4	-9.9
Nastapoca	137.2	23.8	0.17	-0.9**	-20.4
Nelson-Churchill	99.8	16.2	0.16	0.0	1.2
Nottaway	177.8	30.5	0.17	-0.6	-16.1
Pontax	176.7	36.7	0.20	-1.4**	-34.7
Rupert	197.6	34.2	0.17	-0.7**	-20.5
Seal	162.5	41.8	0.25	0.2	6.6
Severn	144.0	27.9	0.19	-1.4**	-27.0
Thlewiaza	141.9	31.8	0.22	-0.3	-8.8
Winisk	143.0	28.3	0.19	-1.4**	-26.8
All watersheds	**126.3**	**21.8**	**0.17**	**-0.4****	**-11.7**

** denotes statistically significant trends ($p<0.05$)

For the overall gauged area (2.50×10^6 km^2), the mean annual SWE_{max} is 126.3 mm with a standard deviation of 21.8 mm and a coefficient of variation of 0.17. Figure 8 illustrates the trend in the total annual SWE_{max} of 20 watersheds of HB during water years 1980 to 2013. The plot shows that the total annual SWE_{max} of HB is decreasing over the period of study, with a significant slope of -0.4 mm yr^{-1}. For the entire HB region, it represents a decrease of 15.3 mm $(34\ yr)^{-1}$ of SWE_{max}. The overall annual maximum SWE_{max} in HB of 169.9 mm occurred in 1997,

and the total annual minimum SWE_{max} of 94.2 mm occurred in 2010. Over the study period, the percent change in the SWE_{max} of 18 rivers is negative. By 2013, the total annual SWE_{max} in HB has decreased by 11.7 % from its value in 1980.

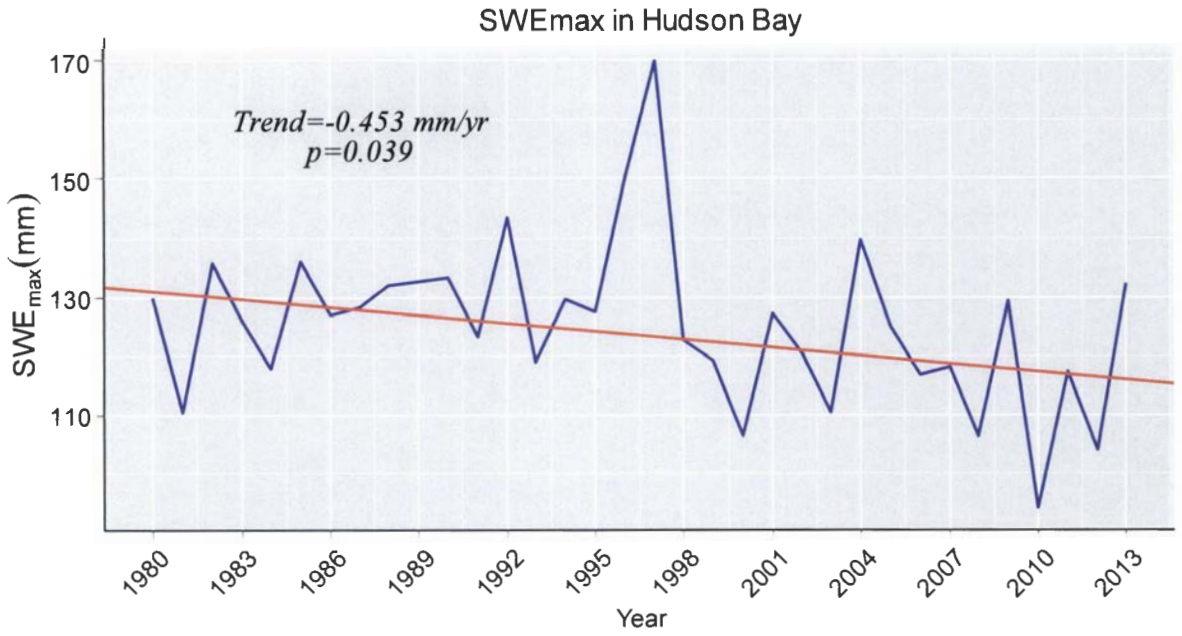

Figure 8. Temporal evolution of the total annual SWE_{max} in 20 Hudson Bay watersheds during water years 1980 to 2013. The red solid line denotes the Kendall-Theil Robust Line.

The annual SWE_{max} for each of the 20 HB watersheds is shown in Figure 9. Out of the 20 watersheds, 18 show a decreasing trend of the annual SWE_{max} with 10 of them being statistically significant (p<0.05): Attawaspikat, Broadback, Chesterfield Inlet, Harricana, Hayes, Nastapoca, Pontax, Rupert, Severn and Winisk.

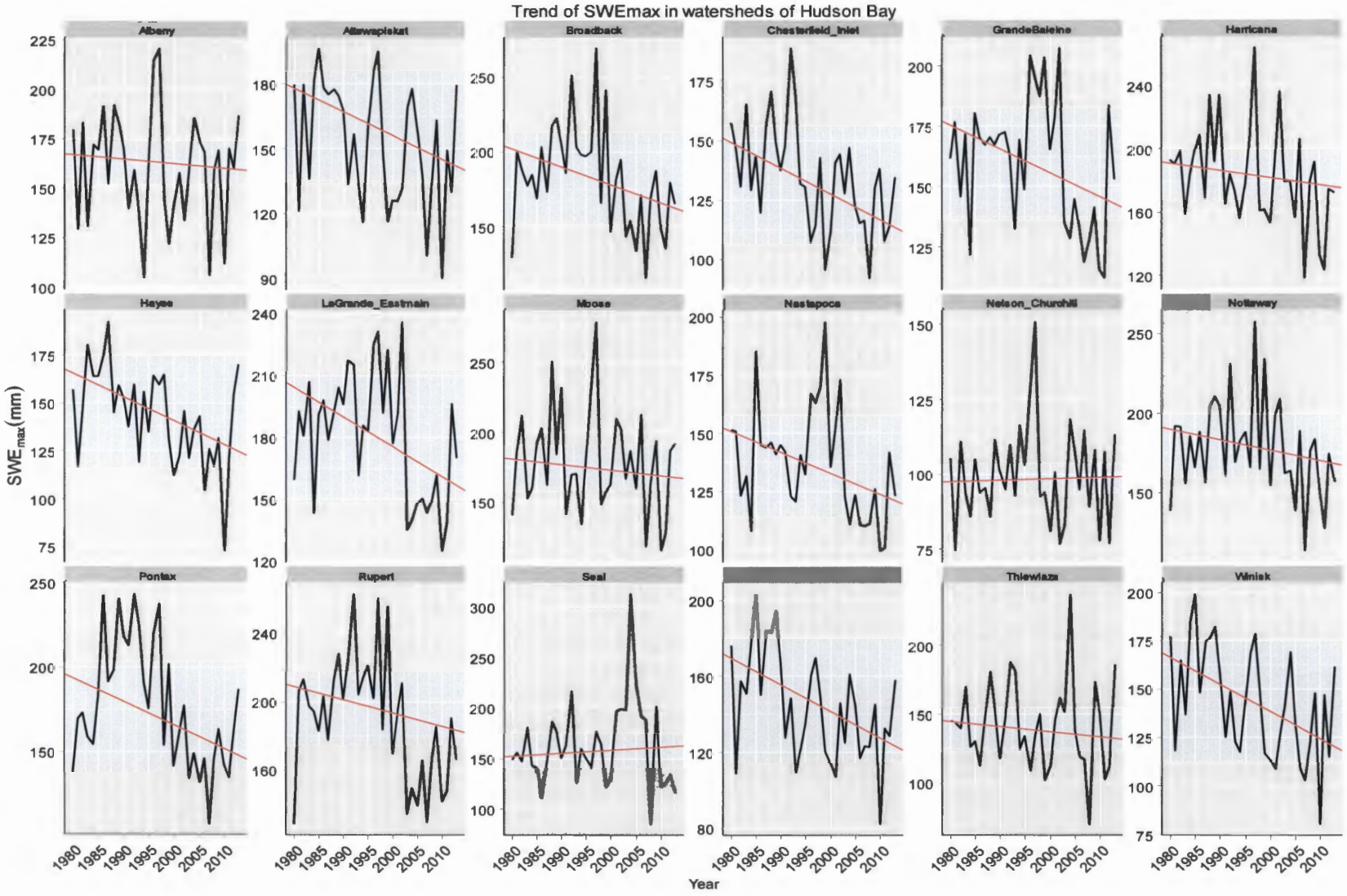

Figure 9. Temporal evolution of the annual SWE_{max} in 20 Hudson Bay watersheds during water years 1980 to 2013. The red solid lines denote the Kendall-Theil Robust Lines. Note: The scale for SWE_{max} varies in each panel.

5.2.1 Comparison of SWE_{max} between Eastern and Western Hudson Bay

On comparing SWE_{max} between eastern and western HB over the period of 34 years, the eastern HB that comprises nine river basins has a mean annual SWE_{max} of 178.5 mm. The western HB with 11 river basins has a mean annual SWE_{max} of 118.1 mm. Table 4 provides the annual SWE_{max} statistics of eastern and western HB. The total SWE_{max} in the eastern and western parts of HB shows a decreasing trend with a slope of -1.2 mm yr^{-1} and -0.3 mm yr^{-1}, respectively where it is statistically significant only for eastern HB. By 2013, the total annual SWE_{max} in eastern and western HB has decreased by 26.5% and 8.3% from its value in 1980, respectively. For eastern and western HB, it represents a decrease of 37.4 mm $(34\ yr)^{-1}$ and 10.2 mm $(34\ yr)^{-1}$ in SWE_{max}, respectively, over a period of 34 years. Figure 10 illustrates the 1980 to 2013 time series plots of total SWE_{max} into eastern and western HB. Both the eastern and western basins show similar patterns in annual SWE_{max} with maximum values in 1997 and minimum values in 2010.

Table 4. The 1980 to 2013 annual mean, standard deviation (SD), coefficient of variation (CV), and trend in SWE_{max} for eastern and western Hudson Bay.

Region of Hudson Bay	Total Gauged Area (km^2)	Annual SWE_{max} Statistics				
		Mean (mm)	SD mm)	CV	Linear Trend (mm yr^{-1})	Percent Change(%)
Eastern	339,390	178.5	30.2	0.16	-1.2**	-26.5
Western	2,170,140	118.1	20.5	0.17	-0.3	-8.3

** denotes statistically significant trends ($p<0.05$)

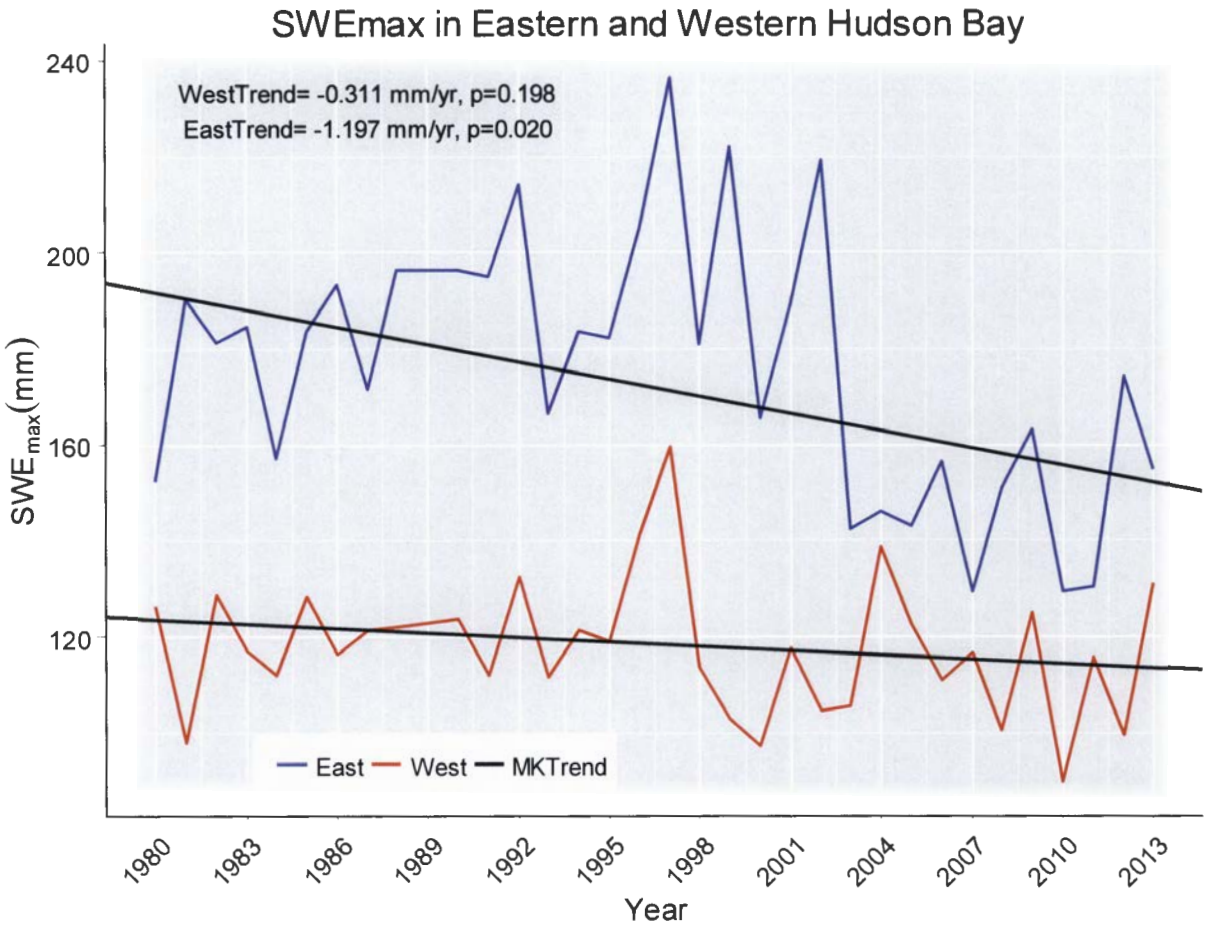

Figure 10.Temporal evolution of the total annual SWEmax in eastern and western Hudson Bay river basins during 1980 to 2013. The solid black lines denote the Kendall-Theil Robust Lines.

5.2.2 Comparison of SWE_{max} between Regulated and Unregulated Hudson Bay Rivers

The regulated and unregulated basins that comprise SWE_{max} from five and 15 rivers have a mean annual SWE_{max} of 111.8 mm and 152.0 mm, respectively. Table 5 provides the annual SWE_{max} statistics of regulated and unregulated basins of HB. The total SWE_{max} in the regulated basins show a decreasing trend with a slope of -1.1 mm yr^{-1} while the unregulated basins show a relatively lower decreasing trend with a slope of -0.8 mm yr^{-1} that is statistically significant. By 2013, the total annual SWE_{max} in regulated and unregulated basins of HB has decreased by

33.6% and 18.1%, respectively from its value in 1980. For the regulated and unregulated basins, it represents a decrease of 37.4 mm $(34\ yr)^{-1}$ and 27.2 mm $(34\ yr)^{-1}$ SWE_{max}, respectively over the study period. Figure 11 illustrates the 1980 to 2013 time series plots of total SWE_{max} in the regulated and unregulated basins of HB. Both the regulated and unregulated basins show similar patterns in annual SWE_{max} with maximum values in 1997 and minimum values in 2010.

Table 5. The 1980 to 2013 annual mean, standard deviation (SD), coefficient of variation (CV), and trend in river runoff for regulated and unregulated rivers of Hudson Bay.

Region of Hudson Bay	Total Gauged Area (km^2)	Annual SWE_{max} Statistics				
		Mean (mm)	SD (mm)	CV	Linear Trend ($mm\ yr^{-1}$)	Percent Change(%)
Regulated	1,605,830	111.8	18.7	0.16	-1.1	-33.6
Unregulated	903,700	152.0	27.4	0.18	-0.8**	-18.1

** denotes statistically significant trends ($p<0.05$)

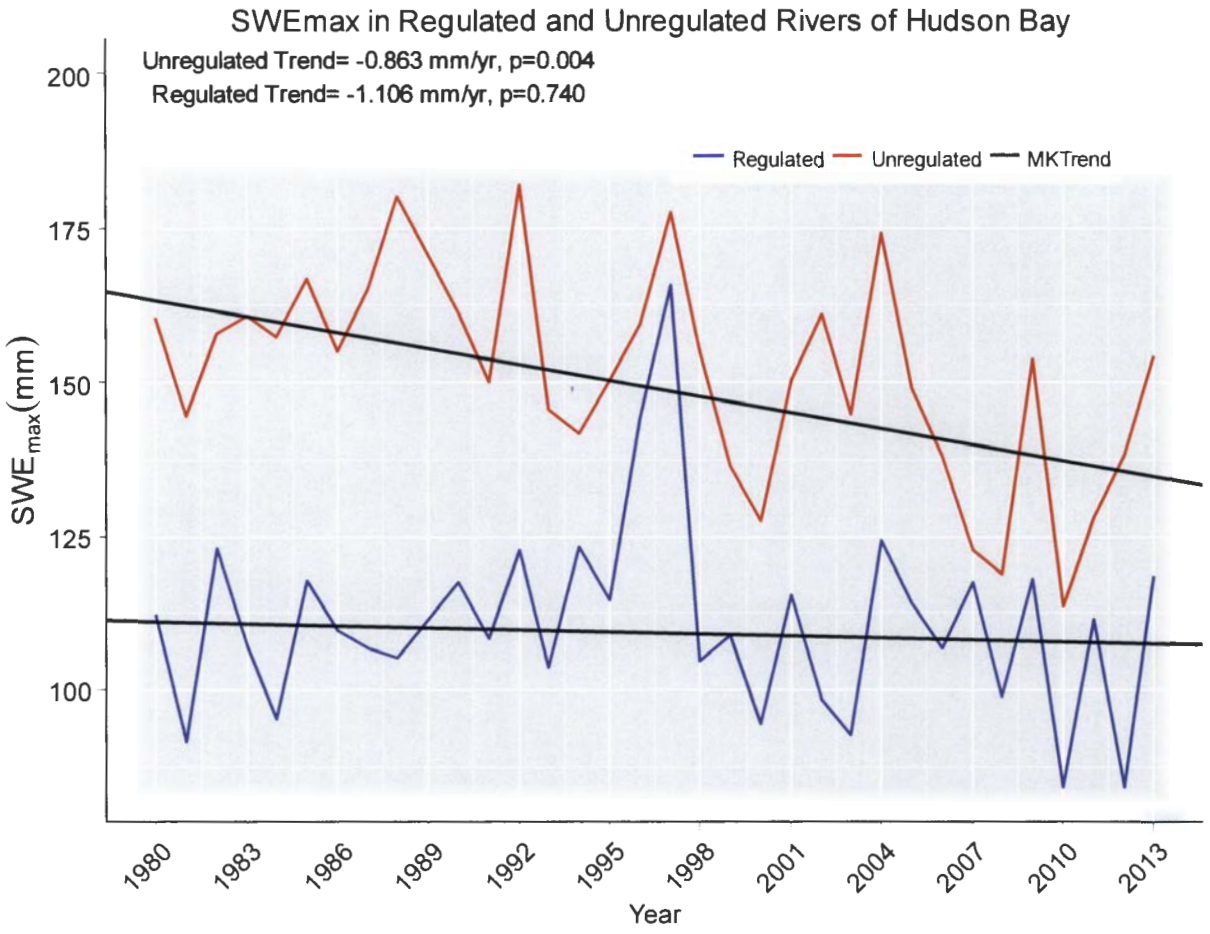

Figure 11. Temporal evolution of the total annual SWE_{max} in regulated and unregulated Hudson Bay river basins from 1980 to 2013. The solid black lines denote the Kendall-Theil Robust Lines.

5.3. Characteristics and Trends of Runoff in Hudson Bay Rivers

The mean, standard deviation and coefficient of variation in annual runoff of the 20 rivers flowing into Hudson Bay are presented in Table 6. The linear trends in annual runoff for each river with slopes and percentage change over the water years 1980 to 2013 are also included in the table. The analysis shows that the relatively small Nastapoca River exhibits a substantially high runoff productivity (692.6 mm) annually to HB. Other rivers that provide a significant amount of runoff to HB are the Rupert, La Grande-Eastmain, Broadback and Nottaway Rivers.

Note that the runoff value is constant in the Severn River in the middle of the study period as there exists a long gap that is in-filled (see section 4.1.3). However, this does not greatly influence the trend analysis of the river in this case because of the in-filling strategy and location of the gaps.

Table 6. The 1980 to 2013 annual mean, standard deviation (SD), coefficient of variation (CV), trend, and percent change in runoff for the 20 rivers of interest. Note that the runoff extends only until 2004 and 2006 for the Harricana and Rupert Rivers, respectively.

Rivers	Annual Runoff Statistics				
	Mean (mm)	SD (mm)	CV	Linear Trend ($mm\ yr^{-1}yr^{-1}$)	Percent Change (%)
Albany	267.3	60.0	0.22	2.0	32.9
Attawapiskat	302.3	88.8	0.29	2.5	30.4
Broadback	577.0	70.9	0.12	2.6**	14.8
Chesterfield Inlet	191.0	32.8	0.17	0.2	5.9
Grande Baleine	435.1	47.7	0.11	-1.2	-8.3
Harricana	516.8	66.8	0.12	-1.1	-6.4
Hayes	188.0	51.8	0.28	0.0	0.0
La Grande-Eastmain	582.1	73.6	0.12	3.3**	20.5
Moose	388.6	67.0	0.17	0.1	0.9
Nastapoca	692.6	75.0	0.11	-3.9	-17.0
Nelson-Churchill	84.3	20.4	0.24	1.1**	48.3
Nottaway	550.0	82.7	0.15	1.3	7.1
Pontax	513.4	70.3	0.14	-0.2	-1.8
Rupert	638.9	53.5	0.08	1.3	5.8
Seal	242.2	44.2	0.18	0.4	7.3
Severn	222.6	49.2	0.22	1.3**	27.0
Thlewiaza	254.1	36.7	0.14	0.5	9.2
Winisk	270.0	83.2	0.31	1.6	22.1
All watersheds	**206.2**	**37.6**	**0.21**	**1.0****	**17.4**

** denotes statistically significant trends ($p<0.05$)

For the overall gauged area (2.50×10^6 km^2), the mean annual runoff is 206.2 mm with a standard deviation of 37.6 mm and a coefficient of variation of 0.21. This equates to a mean annual streamflow rate of 16,409 m^3 s^{-1}. Figure 12 illustrates the trend in the total annual runoff of 20 rivers draining into HB during 1980 to 2013. The total annual runoff into HB is increasing over the period of study, with a significant slope of 1.0 mm yr^{-1} yr^{-1}, which represents an increase of 34.3 mm $(34\ yr)^{-1}$. The total annual maximum runoff into HB is 244.6 mm that occurred in 2005, and the total annual minimum runoff is 173.5 mm that occurred in 1982. Over the period of 1980 to 2013, the percent change in runoff is positive for 13 of the rivers with four of them being statistically significant: Broadback, LaGrande-Eastmain, Nelson-Churchill and Severn Rivers and negative for the remaining rivers. By 2013, the total annual freshwater discharge into HB has increased by 17.4% from its value in 1980. The annual runoff in each river that drains into HB is shown in Figure 13.

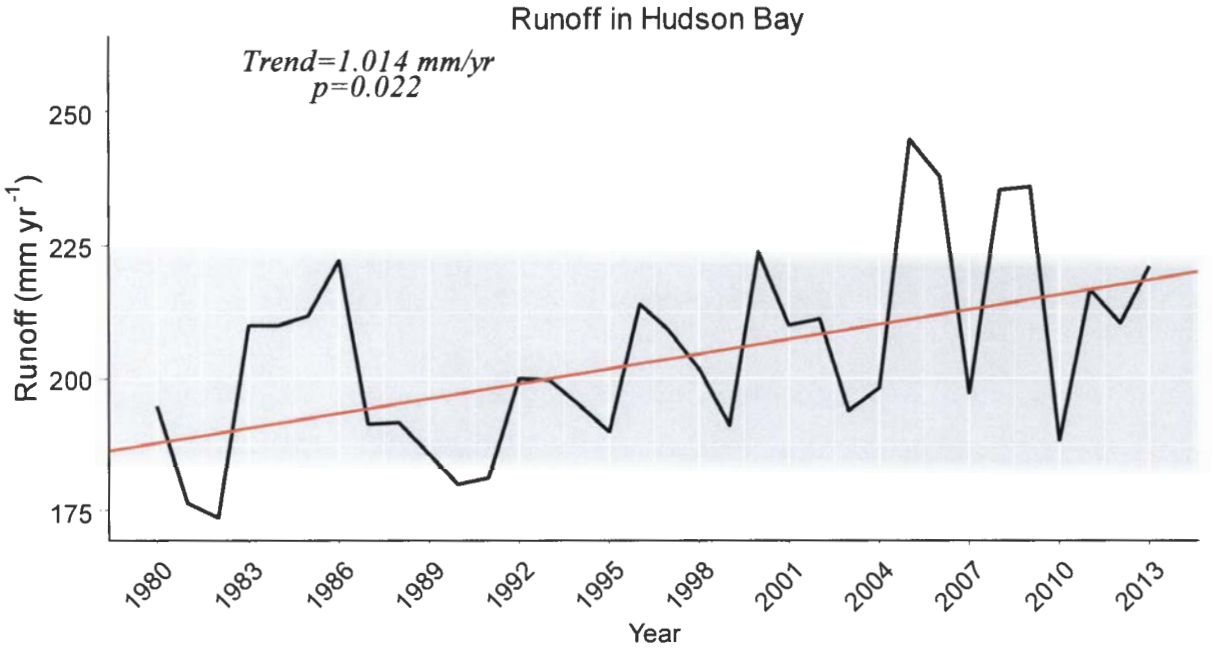

Figure 12. Temporal evolution of the total annual runoff of 20 rivers that drain into Hudson Bay during water years 1980 to 2013. The red solid line denotes the Kendall-Theil Robust Line.

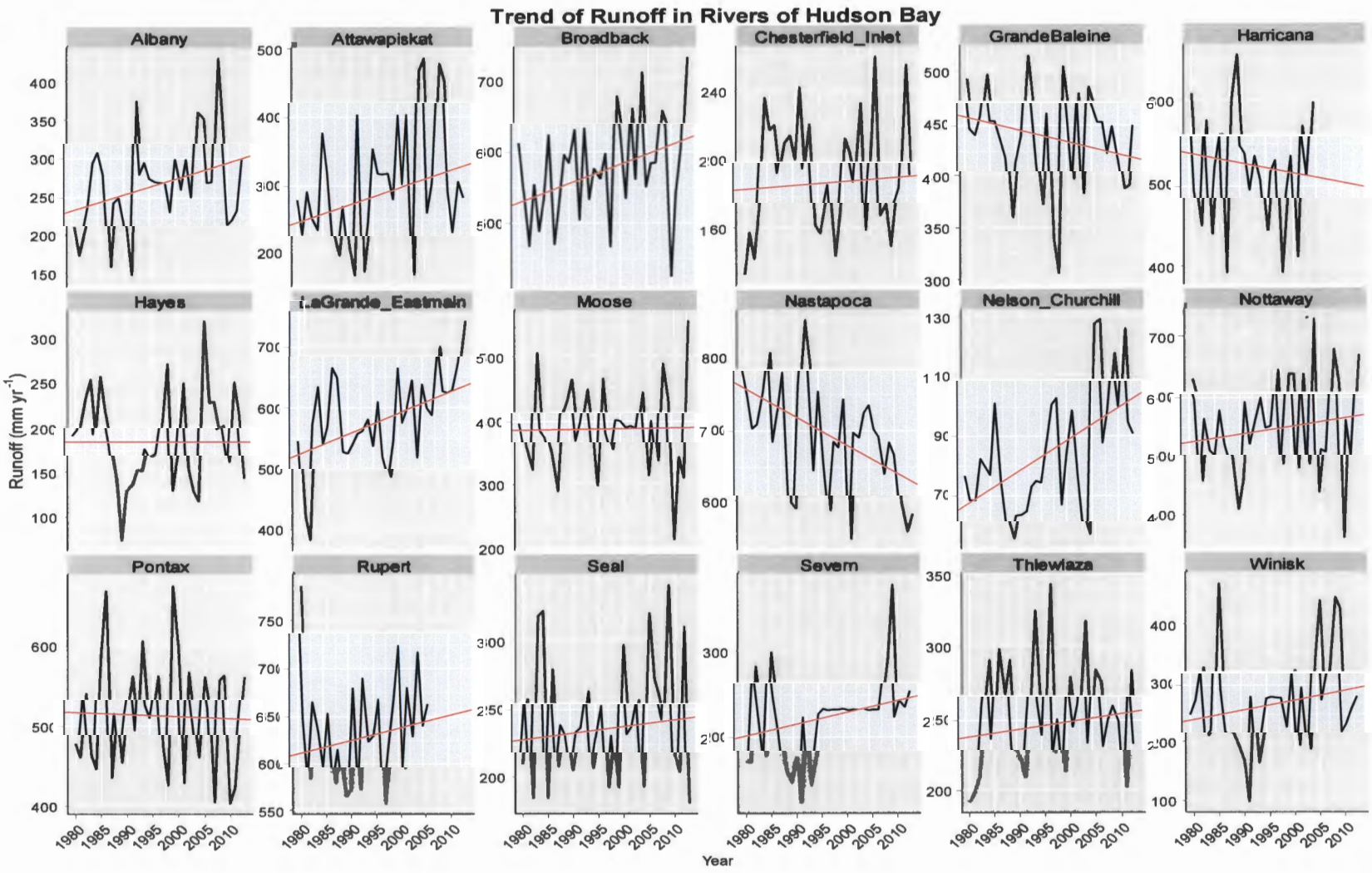

Figure 13. Temporal evolution of the annual runoff in 20 rivers that drain into Hudson Bay during water years 1980 to 2013 (except the end year is 2004 and 2006 for the Harricana and Rupert Rivers, respectively). The red solid lines denote the Kendall-Theil Robust Lines. Note that there exists a long gap in the Severn that is in-filled (see section 4.1.3) and the scale for runoff varies in each panel.

5.3.1 Comparison of Runoff between Eastern and Western Hudson Bay

The Eastern Hudson Bay with an area of 339,390 km^2 and comprising discharge from nine rivers has mean annual runoff of 565.1 mm while western HB with an area of 2,170,140 km^2 from 11 river basins has mean annual runoff of 143.9 mm. Table 7 provides the annual runoff statistics of eastern and western HB. The total runoff in the eastern and western parts shows a statistically significant increasing trend with a slope of 1.2 mm yr^{-1} yr^{-1} and 1.0 mm yr^{-1} yr^{-1}, respectively. By 2013, the total annual freshwater runoff into eastern and western HB has increased by 6.8% and 26.9%, respectively from its value in 1980. Figure 14 illustrates the 1980 to 2013 time series plots of total inflow into eastern and western HB. For the eastern and western part, it represents an increase of 40.8 mm $(34\ yr)^{-1}$ and 34.0 mm $(34\ yr)^{-1}$ runoff, respectively.

Table 7. The 1980 to 2013 annual mean, standard deviation (SD), coefficient of variation (CV), and trend in river runoff for eastern and western Hudson Bay.

Region of Hudson Bay	Total Gauged Area (km^2)	Annual Runoff Statistics				
		Mean (mm)	SD (mm)	CV	Linear Trend (mm yr^{-1} yr^{-1})	Percent Change (%)
Eastern	339,390	565.1	69.3	0.12	1.2**	6.8
Western	2,170,140	143.9	32.1	0.23	1.0**	26.9

** denotes statistically significant trends ($p<0.05$)

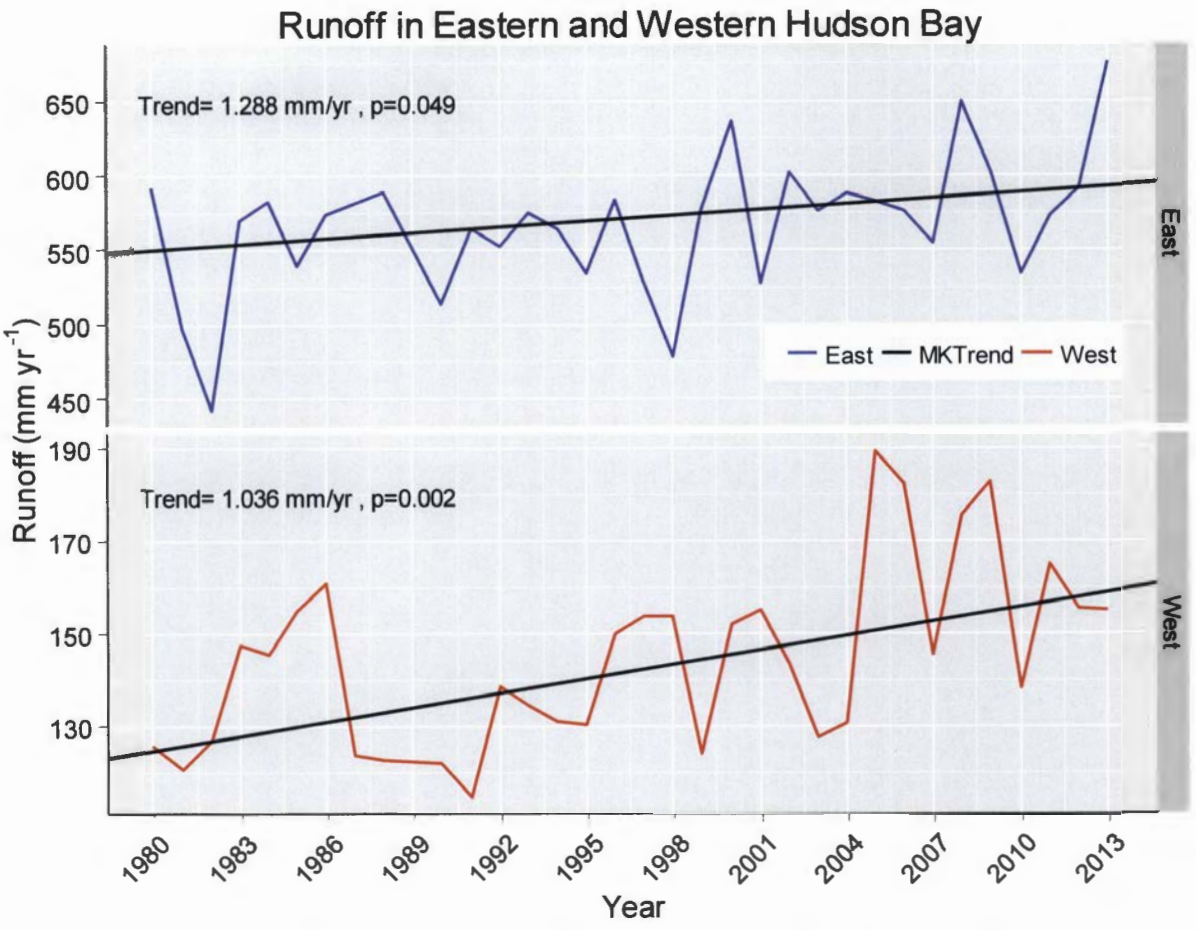

Figure 14. Temporal evolution of the total annual runoff in eastern and western Hudson Bay rivers during water years 1980 to 2013. The black lines denote the Kendall-Theil Robust Lines.

5.3.2 Comparison of Runoff between Regulated and Unregulated Hudson Bay Rivers

On comparing inflows between regulated and unregulated rivers of Hudson Bay over a period of 34 years, the regulated basins with a larger area of 1,605,830 km^2 comprise runoff from five rivers with a mean annual runoff of 156.5 mm. The unregulated basins with an area of 903,700 km^2 comprise runoff from 15 rivers with a mean annual runoff of 296.6 mm. Table 8 provides the annual runoff statistics of regulated and unregulated basins of HB. The total runoff in the regulated basins shows a statistically significant increasing trend with a slope of 1.3 mm yr^{-1} yr^{-1}

while the runoff in unregulated basins shows a relatively lower increasing trend with a slope of 0.4 mm yr^{-1} yr^{-1} that is not statistically significant. By 2013, the total annual freshwater discharge into both regulated and unregulated basins of HB has increased by 30.1% and 4.8%, respectively from its value in 1980. For the regulated and unregulated regions of HB, it represents an increase of 44.2 mm $(34\ yr)^{-1}$ and 13.6 mm $(34\ yr)^{-1}$ in runoff, respectively over a period of 34 years. Figure 15 illustrates the 1980 to 2013 time series plots of total inflow into regulated and unregulated basins of HB. Both the regulated and unregulated basins show similar patterns in annual runoff with maximum values during 2005 to 2006.

Table 8. The 1980 to 2013 annual mean, standard deviation (SD), coefficient of variation (CV), and trend in river runoff for regulated and unregulated rivers of Hudson Bay.

Region of Hudson Bay	Total Gauged Area (km^2)	Annual Runoff Statistics				
		Mean (mm)	SD (mm)	CV	Linear Trend (mm yr^{-1} yr^{-1})	Percent Change (%)
Regulated	1,605,830	156.5	28.9	0.22	1.3**	30.1
Unregulated	903,700	296.6	53.4	0.20	0.4	4.8

** denotes statistically significant trends ($p<0.05$)

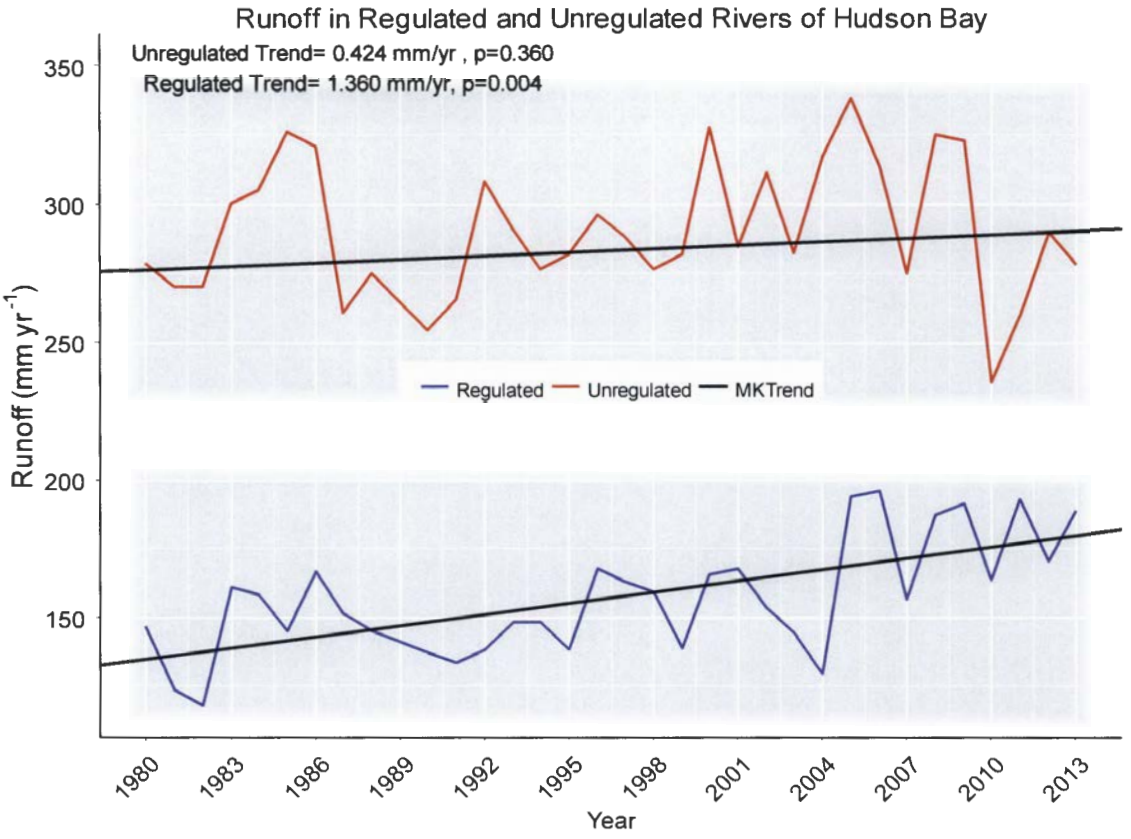

Figure 15. Temporal evolution of the total annual runoff in regulated and unregulated Hudson Bay rivers during 1980 to 2013. The black lines denote the Kendall-Theil Robust Lines.

5.4. Characteristics and Trends of R_{SR} in Hudson Bay Rivers

The linear trends in annual R_{SR} (the ratio of SWE_{max} to runoff) for each river are presented in Figure 16. The values of trends and *p*-values are presented in Table 9. This analysis shows that out of the 20 rivers, 19 show a decreasing trend of the annual R_{SR} with nine of them being statistically significant.

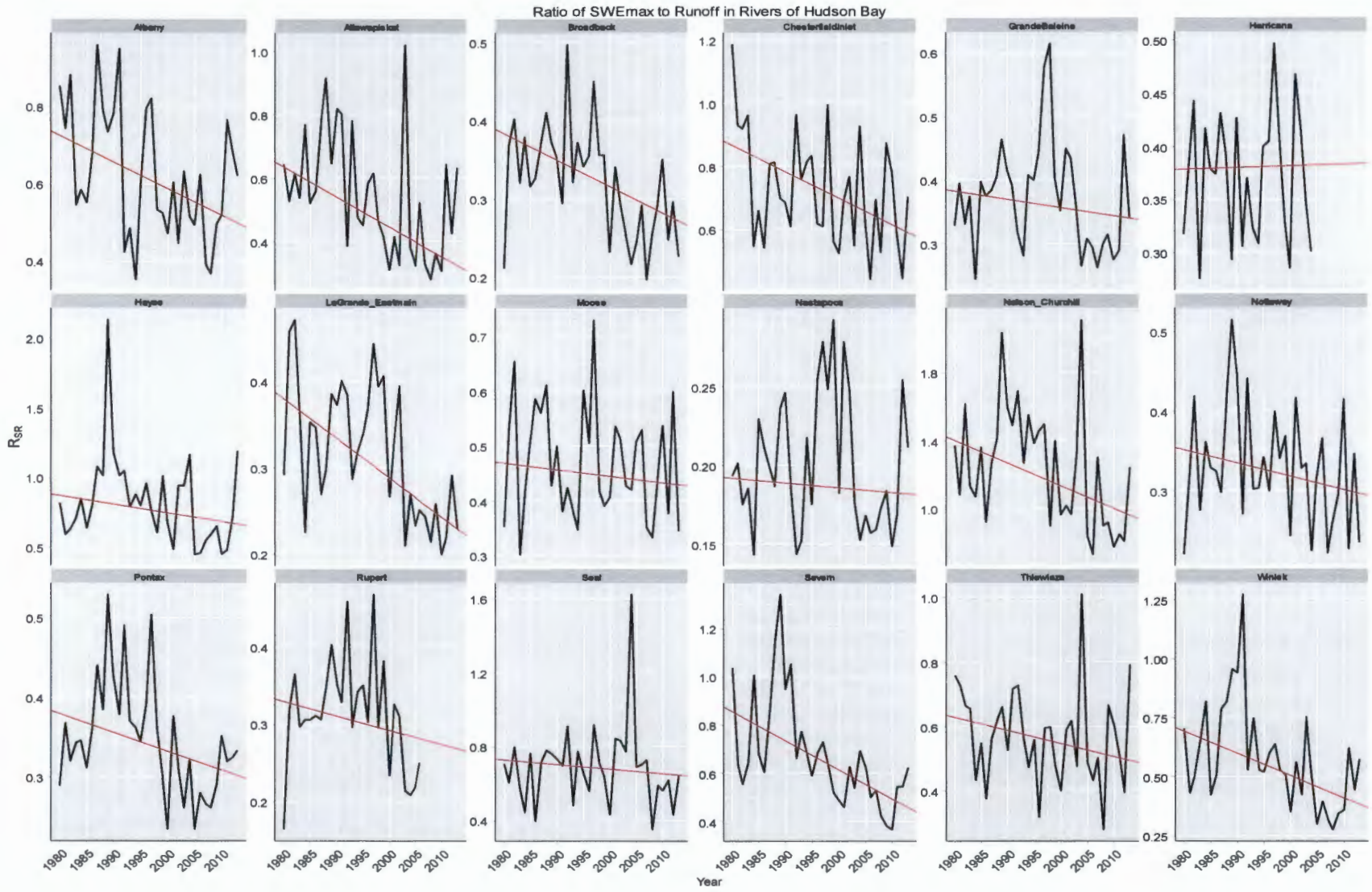

Figure 16. Temporal evolution of the annual R_{SR} in 20 Hudson Bay watersheds during water years 1980 to 2013. The red solid line denotes the Kendall-Theil Robust Line. Note: The scale for R_{SR} varies in each panel.

Table 9. Trends of R_{SR} during 1980 to 2013 in 20 Hudson Bay rivers with their *p*-values. Note that R_{SR} time series extend only until 2004 and 2006 for the Harricana and Rupert Rivers, respectively.

River	Trend (% yr^{-1})	*p*-value
Albany	-0.684**	0.035
Attawapiskat	-0.946**	0.005
Broadback	-0.337**	0.004
Chesterfield Inlet	-0.833**	0.035
Grande Baleine	-0.133	0.441
Harricana	0.014	1.000
Hayes	-0.627	0.131
La Grande-Eastmain	-0.456**	0.002
Moose	-0.120	0.477
Nastapoca	-0.031	0.767
Nelson-Churchill	-1.329**	0.007
Nottaway	-0.167	0.248
Pontax	-0.236**	0.038
Rupert	-0.185	0.260
Seal	-0.247	0.406
Severn	-1.204**	0.000
Thlewiaza	-0.406	0.173
Winisk	-0.936**	0.006
Total	**-0.47****	**0.004**

** denotes statistically significant trends ($p<0.05$)

Figure 17 illustrates the trend in the total annual R_{SR} of 20 Hudson Bay watersheds during 1980 to 2013. It shows that the total annual R_{SR} value of HB is decreasing with a statistically significant slope of 0.4% yr^{-1}. Over the study period it has decreased by 15.9 % $(34\ yr)^{-1}$. The total annual maximum R_{SR} in HB of 0.8 occurred in 1987, and the total annual minimum R_{SR} of 0.4 occurred in 2008.

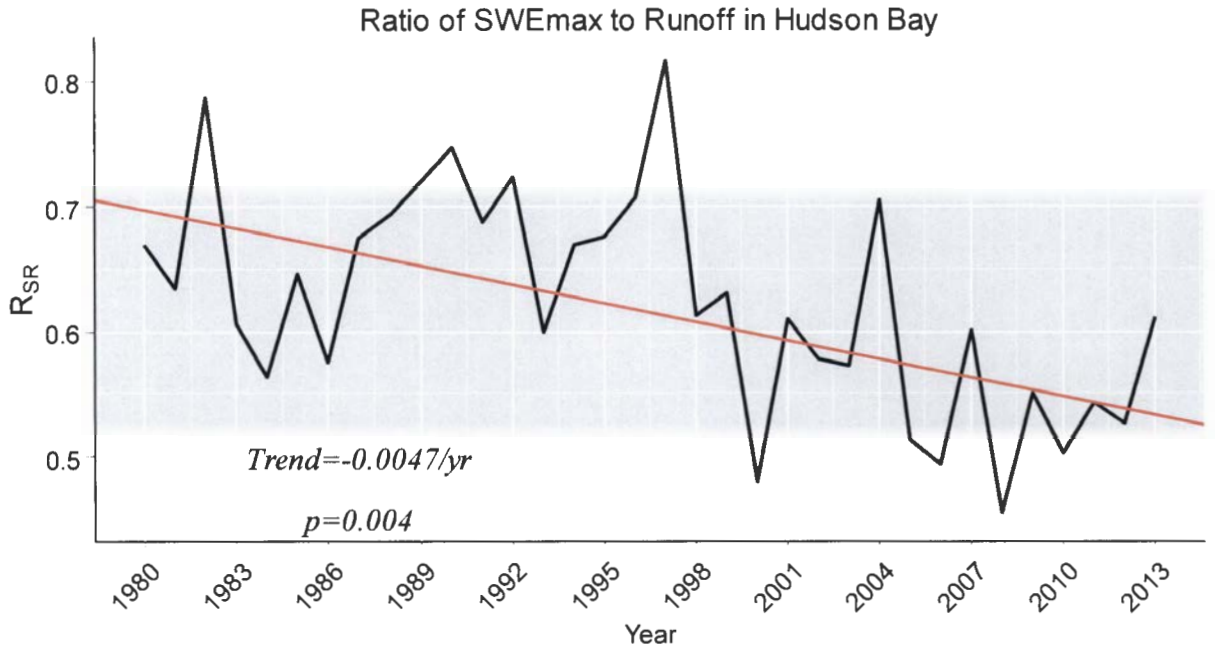

Figure 17. Temporal evolution of the total annual R_{SR} in 20 Hudson Bay rivers during water years 1980 to 2013. The red solid line denotes the Kendall-Theil Robust Line.

5.4.1 Comparison of R_{SR} between Eastern and Western Hudson Bay

On comparing R_{SR} between western and eastern Hudson Bay over the period of 34 years, the eastern HB that comprises nine rivers has an R_{SR} value decreasing by 0.3 % yr^{-1}. In western HB the R_{SR} from 11 rivers has decreased by 0.8% yr^{-1} that is statistically significant. For the eastern and western regions of HB, it represents a decrease of 10.2 % $(34\ yr)^{-1}$ and 27.2% $(34\ yr)^{-1}$ in R_{SR}, respectively. Figure 18 illustrates the 1980 to 2013 time series plots of total R_{SR} into eastern and western HB.

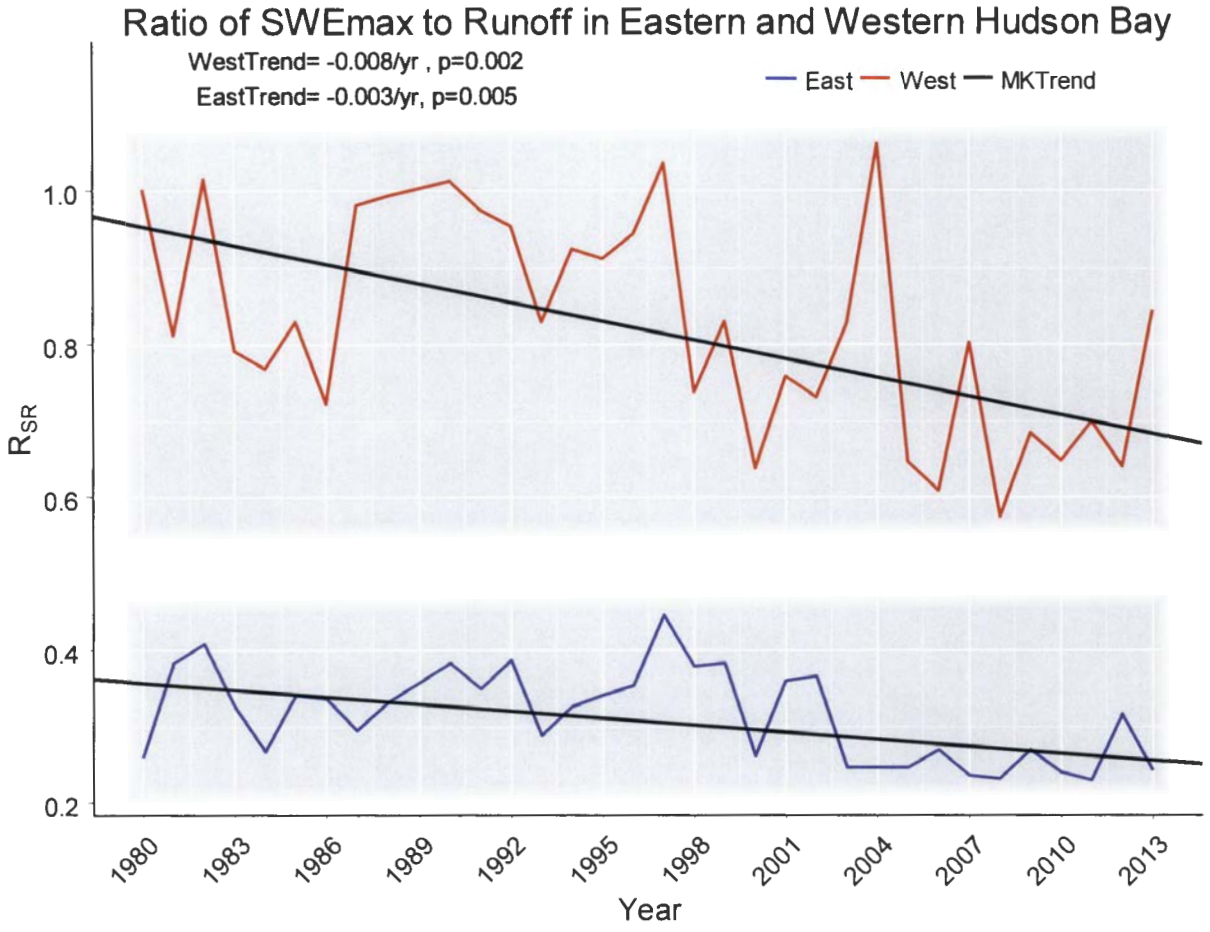

Figure 18. Temporal evolution of the total annual R_{SR} in eastern and western Hudson Bay river basins during 1980 to 2013. The black lines denote the Kendall-Theil Robust Lines.

5.4.2 Comparison of R_{SR} between Regulated and Unregulated Rivers of Hudson Bay

On comparing R_{SR} between regulated and unregulated basins of Hudson Bay over a period of 34 years, the regulated basins of HB that comprise the ratio of SWE_{max} to runoff from five rivers have an R_{SR} value decreasing with a significant slope of 0.6% yr^{-1}. The unregulated basins with 15 rivers have a decreasing mean annual R_{SR} of 0.3% yr^{-1} that is statistically significant. For the regulated and unregulated basins of HB, this represents a decrease of 20.4 % $(34\ yr)^{-1}$ and 10.2% $(34\ yr)^{-1}$ in R_{SR}, respectively. Figure 19 illustrates the 1980 to 2013 time series plots of total R_{SR}

into regulated and unregulated basins of HB. Both the regulated and unregulated basins show similar patterns of annual R_{SR} over the study period.

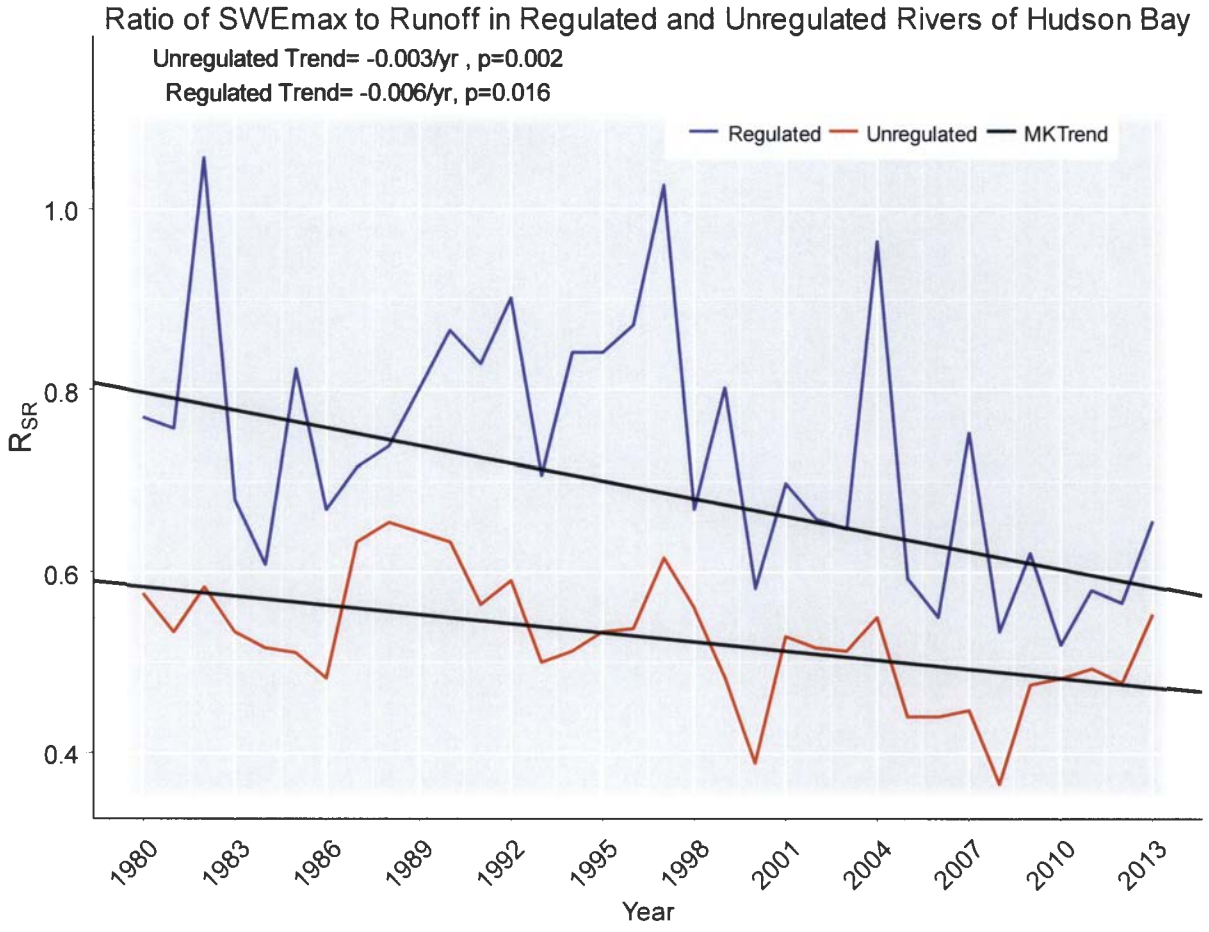

Figure 19. Temporal evolution of the total annual R_{SR} in regulated and unregulated Hudson Bay river basins from 1980 to 2013. The black lines denote the Kendall-Theil Robust Lines.

5.5. Overall Contribution of Snow to Runoff Generation

The contribution of snow to runoff generation for 20 Hudson Bay rivers as given by the ratio of SWE_{max} to runoff (R) for each river is presented in Table 10. The analysis shows that the Nelson-Churchill River with the largest basin area (1,366,400 km^2) and lowest SWE_{max} (99.8 mm) and

runoff (84.3 mm) contributes the highest in snow to runoff generation. Further, the Nastapoca River with the second smallest basin area (12,500 km^2) and relatively high SWE_{max} (137.2 mm) and runoff (692.6 mm) contributes the least in snow to runoff generation in HB. Overall, during the study period of 34 years from 1980 to 2013, the contribution of snow to runoff generation in 20 HB rivers is 61.5% and it has decreased by 20.6% from its value in 1980.

Table 10. The values of SWE_{max}, runoff and their ratio during 1980 to 2013 in the rivers of Hudson Bay showing overall contribution of snow to runoff generation. Note that all values for the Harricana and Rupert Rivers extend only until 2004 and 2006, respectively.

River	SWE_{max} (mm)	Runoff (mm)	Ratio (%)
Albany	159.9	267.3	59.8
Attawapiskat	152.4	302.3	50.4
Broadback	182.6	577.0	31.6
Chesterfield Inlet	134.5	191.0	70.4
Grande Baleine	159.5	435.1	36.6
Harricana	190.0	516.8	36.7
Hayes	142.9	188.0	76.0
La Grande-Eastmain	180.7	582.1	31.0
Moose	179.2	388.6	46.1
Nastapoca	137.2	692.6	19.8
Nelson-Churchill	99.8	84.3	118.3
Nottaway	177.8	550.0	32.3
Pontax	176.7	513.4	34.4
Rupert	197.6	638.9	30.9
Seal	162.5	242.2	67.1
Severn	144.0	222.6	64.6
Thlewiaza	141.9	254.1	55.8
Winisk	143.0	270.0	52.9
Total	**126.2**	**205.1**	**61.5**

5.6. Trends in Daily Runoff

Trends in daily runoff are analyzed to observe changes in the annual hydrograph including possible shifts in the spring freshet. Figure 20 shows plots of daily runoff trends for the unregulated rivers. A seven-day moving average curve is added to smooth out fluctuations in daily runoff trends. For some of the rivers (Albany, Attawaspikat, Nottaway, and Pontax) a prominent shift to an earlier timing of the spring freshet is observed in between the last week of April and the third week of June. Further rivers such as the Broadback, Grande Baleine, Pontax, Hayes, Rupert and Seal show a higher runoff trends during winter.

Changes in the mean annual hydrograph of the two periods are shown in Figure 21. On average, higher magnitude of spring runoff is observed in the first half of the study period (1980 to 1996) in 11 out of 14 rivers than in the latter half period (1997 to 2013). This corresponds to the prominently decreasing SWE_{max} in the latter study period (see Figure 9). Some of the rivers such as the Albany, Nottaway, Broadback and Hayes exhibit an earlier start of the spring freshet in the latter half rather than the first half of the study period. This is shown by the earlier appearance of spring runoff during the latter period of study in the annual cycle of daily mean runoff (see Figure 21). In addition, in the latter half study period, there is relatively high runoff during the first three months of a hydrological year from October to December in nine of the 14 rivers showing change in the hydrological conditions of the rivers. Therefore, such changes in the hydrological regime of the rivers in the latter half of the study period show that there are changes in the timing of snowmelt onset, impacting the freshwater budget of HB with implications for streamflow timing.

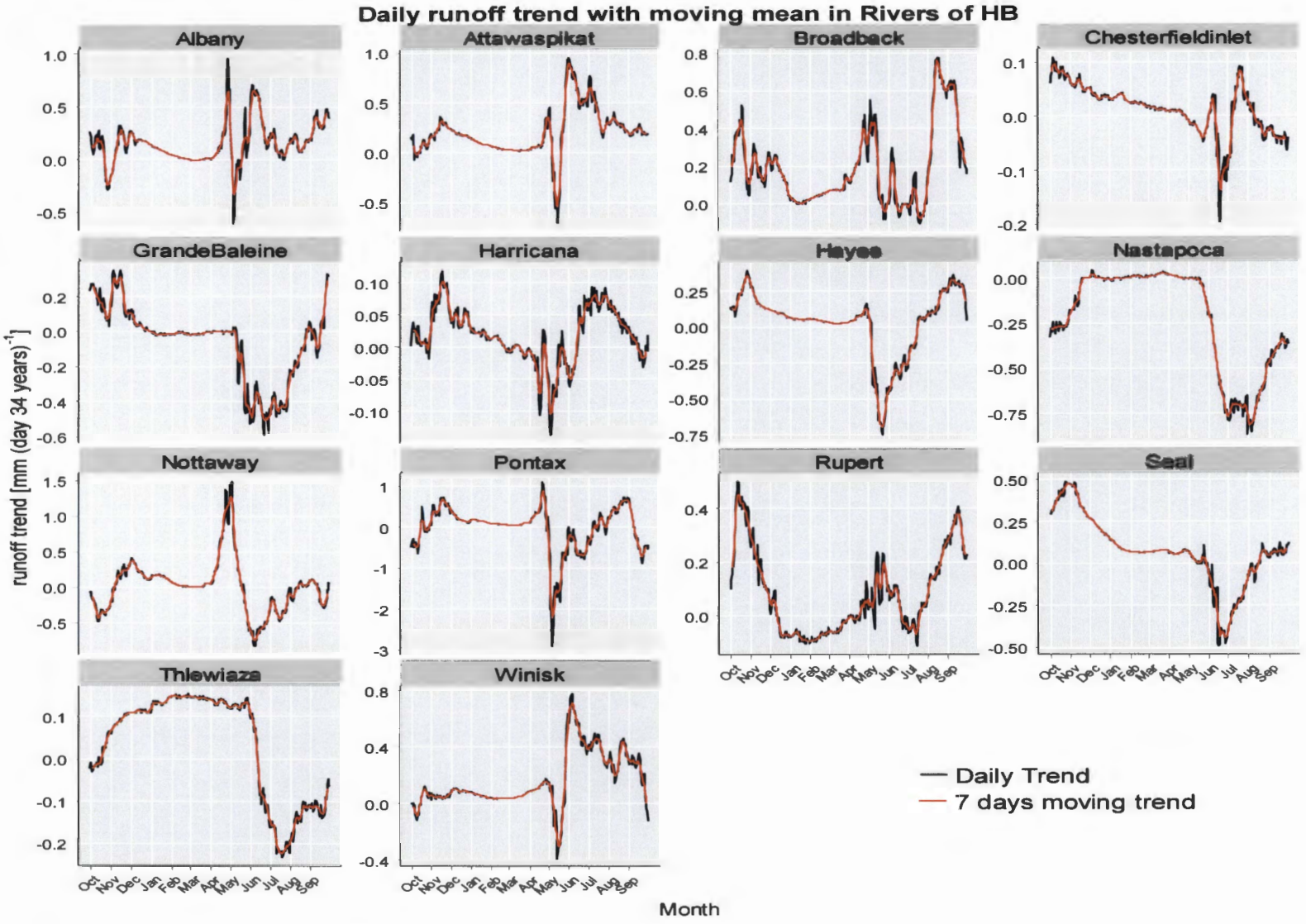

Figure 20. Daily runoff trend in unregulated Hudson Bay rivers during 1980 to 2013. The black lines show the daily trends and the red lines denote the 7-days moving averages. Note: The scale for runoff trend varies in each panel.

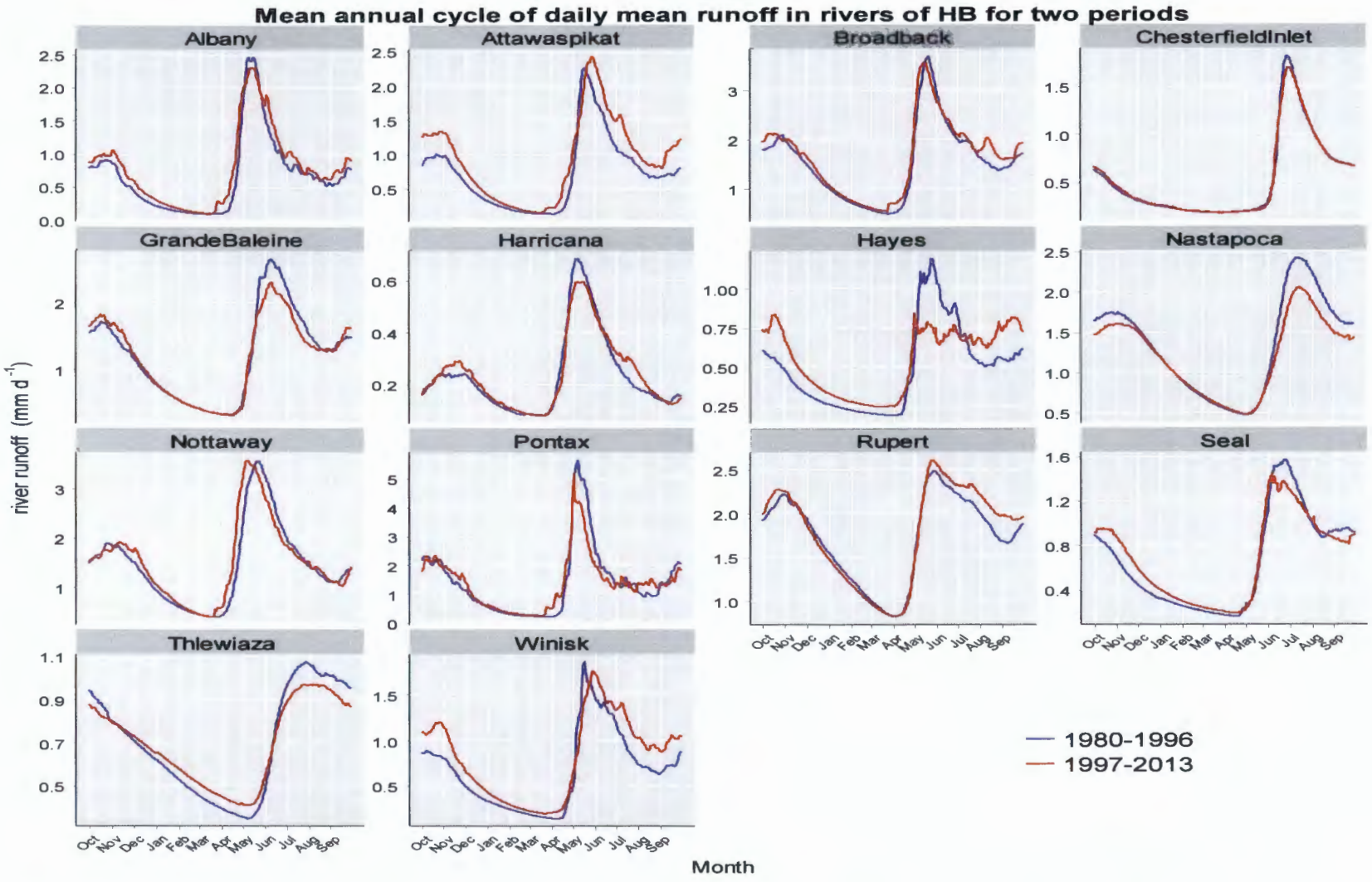

Figure 21. Mean annual cycle of daily runoff in the unregulated Hudson Bay rivers for 1980 to 1996 and 1997 to 2013. Note that the study periods for Rupert is 1980 to 1992 and 1993 to 2006 and Harricana is 1980 to 1991 and 1992 to 2004 due to limited availability of runoff data. Note: The scale for river runoff varies in each panel.

6. Discussion

In this chapter the trends of SWE, runoff and R_{SR} in the Hudson Bay rivers and their impacts in the region are discussed. Further, findings of this study are used to discuss the changing hydrologic conditions of the HB region. The results of this study are supported and contrasted by the findings of other studies. Furthermore, the limitations of the study, and the ecological and social impacts of such changing hydrologic conditions are discussed based on the findings of other studies.

6.1. Change in Snow Condition

Temporal SWE_{max} trends for all of the Hudson Bay drainage basin show a statistically significant decreasing trend of 0.4 mm yr^{-1} within the study period (see Figure 8). These decreasing trends of SWE in HB are consistent with the findings of Liston & Hiemstra (2011) for the pan-Arctic domain and Mote, Hamlet, Clark, & Lettenmaier (2005) for the NH. Further, Takala et al. (2011) estimated the snow mass for March calculated by multiplying SWE values with area during the period of 1982 to 2009 over the NH shows a declining trend of 7% for a period of 30 years that is similar to the findings of this study. The annual maximum SWE_{max} in 1997 may be associated with the winter Pacific/North American (PNA) pattern and the North Atlantic Oscillation (NAO). Zhao, Higuchi, Waller, Auld and Mote (2013) identified a significant correlation between these phenomena and SWE_{max} anomalies in eastern and western Canada. They reported that the largest mean values of SWE_{max} are due to the high frequency of snowstorm occurrences caused by the positive phase of these teleconnection patterns. Further, they also found that the averaged SWE_{max} over central Ontario is highest in the hydrological year 1997 in association with the positive phase of the NAO, similar to the findings of this study. The annual minimum SWE_{max} in 2010 may be associated with a strong El Niño (positive phase of El Niño/Southern

Oscillation) that leads to warmer and drier weather and less snowfall during the winter of a particular year over the HB drainage basin.

The average SWE_{max} is found to be higher on the eastern side of HB than on its western side (see Table 4). The annual mean total precipitation and maximum snow depth in the eastern part of HB is higher than in the western part (see Appendix 1 and 2). Further, the analysis performed by Derksen & MacKay (2006) also shows the monthly averaged SWE during 1979 to 1996 was higher in the eastern part of HB than in the western part. The average SWE_{max} is higher in unregulated basins than in regulated ones (see Table 5) because of the geographical location of the basins in the region of higher annual mean total precipitation and maximum snow depth (see Appendix 1 and 2).

The declining trend in annual SWE_{max} in the HB region may be due to the warming air temperature in the region that decreases the snowfall and causes more precipitation to fall as rainfall. Brown & Mote (2009) and Zhang et al. (2011) observed more precipitation falling in the form of rain across Canada during the period of 1966 to 2007 and 1950 to 2007, respectively. Further, there are studies showing the warming air temperature trends in the HB region. Gagnon & Gough (2002) reported a statistically significant warming trend in spring temperature in a region extending from Manitoba to Québec. In addition, Gagnon & Gough (2005a) found a statistically significant warming air temperature trend during winter and year-round for the period of 1971 to 2001 in most of the region on the HB drainage basin. Air temperatures are increasing at a rate of 0.17°C decade^{-1} (p<0.05) in the Chesterfield Inlet Basin, 0.50°C decade^{-1} (p<0.10) in the Churchill River Basin, and 0.67°C decade^{-1} (p<0.05) in parts of the Moose River Basin. Thistle & Caissie (2013) reported an increase of annual mean temperature by 0.3°C to 0.6°C and 0.6 °C to 1.0°C decade^{-1} in the southern and northern part of Québec. Park, Yabuki, &

Ohata (2012) observed a warming trend in Arctic and sub-Arctic regions with an increasing winter temperature of 0.42°C decade^{-1} from 1979 to 2006.

6.2. Change in Runoff

The temporal runoff trend for Hudson Bay shows a statistically significant increasing value of 1.0 mm yr^{-1} yr^{-1} within the study period (see Figure 12). This increasing trend in HB runoff is consistent with the findings of Déry et al. (2005), Déry, Hernández-Henríquez, Burford, & Wood (2009), Déry, Mlynowski, Hernández-Henríquez, & Straneo (2011), and Gagnon & Gough (2002). Further, this finding is consistent with the Fourth Assessment Report of the Intergovernmental Panel on Climate Change's finding that, in high latitudes, runoff and discharge have generally increased (Hartmann et al., 2013). However, the findings of this study are not consistent with those of Déry & Wood (2005), McClelland, Déry, Peterson, Holmes, & Wood (2006), and Zhang, Harvey, Hogg, & Yuzyk (2001). This may be due to the difference in the study period and the spatial coverage of these studies. Zhang, Harvey, Hogg, & Yuzyk (2001) analyzed the trend of streamflow based on limited record lengths of streamflow data and spatial coverage in the prairies and western Ontario, Québec and the northern part of HB. Further, Déry & Wood (2005) and McClelland, Déry, Peterson, Holmes, & Wood (2006) analyzed the runoff rates during the period of 1964 to 2000. Therefore, such a difference in temporal and spatial scale may lead to variability in total inflow into HB, thereby producing contrasting results.

The maximum annual runoff is observed in 2005 is similar to the findings of Déry, Mlynowski, Hernández-Henríquez, & Straneo (2011). The maximum annual runoff observed in 2005 may be

the consequence of major flooding caused by more precipitation in the Nelson River Basin that intensified the runoff (Flesch & Reuter, 2012; Shein, 2006). The minimum annual runoff observed in 1982 might be the consequence of relatively lower precipitation rates and higher evapotranspiration rates observed in the Arctic drainage system in that particular year (Serreze et al., 2003). Further, an El Niño was very strong that year resulting in warmer temperatures with higher evapotranspiration over HB (Shabbar & Khandekar, 1996).

Higher mean annual runoff is observed in eastern Hudson Bay compared to western HB (see Table 7). There is much more evapotranspiration in the Canadian Prairies than elsewhere in the HB basin (Serreze et al., 2003; Déry et al. 2005). This diminishes runoff productivity in the west that is dominated by the Canadian Prairies, leading to higher runoff in eastern HB generated by more melting of snow than in the western part. The higher average runoff observed in unregulated basins than in regulated ones (see Table 8) might be because the regulated basin is dominated by the wide area of the Nelson River basin that lies in the Canadian Prairies and has low runoff productivity.

The overall increasing trend in runoff in Hudson Bay may be attributed to the warming climate (Labat, Goddéris, Probst, & Guyot, 2004). There are studies showing increasing air temperature trends from 1920 to the late 1990's in the HB region (Gagnon & Gough, 2002; Gagnon & Gough, 2005b; Hochheim, Lukovich, & Barber, 2011; Zhang et al. 2011) and increasing precipitation in the HB region (Mekis & Vincent, 2011; Thistle & Caissie 2013; Zhang et al. 2011). Further, increased precipitation in the form of rain on snow increases runoff of HB.

6.3. Trends in Daily Runoff

Daily runoff trends of unregulated rivers (see Figure 20) show an increasing winter runoff for most of the rivers. Further, earlier spring freshets are observed for some of the rivers of HB. The earlier spring freshet for these rivers is observed on average in the last week of April or in early May. There are many studies showing earlier spring freshets in North America such as Barnett et al. (2005), Déry et al. (2009), Hidalgo et al. (2009), Hodgkins & Dudley (2006), Maurer, Stewart, Bonfils, Duffy, & Cayan (2007), Moore, Harper, & Greenwood (2007), Stewart, Cayan, & Dettinger (2005), and Zhang, Harvey, Hogg, & Yuzyk (2001). Such trends toward an increasing winter runoff and earlier spring freshet may be attributed to the greater likelihood of rain than snow and reduced SWE accumulation combined with the warming spring air temperature recorded in the second half of the 20th century and early 21st century, leading to earlier snowmelt (Arora & Boer, 2001; Hidalgo et al. 2009; Maurer, Stewart, Bonfils, Duffy, & Cayan, 2007; Zhang, Harvey, Hogg & Yuzyk, 2001).

Further, the mean annual cycle of daily runoff of unregulated Hudson Bay rivers (see Figure 21) for two periods shows a change in the hydrological cycle of the rivers. The high magnitude of spring runoff observed in the first half of the study period (1980 to 1996) compared to the latter half period (1997 to 2013) in most of the rivers may be attributed to decreasing SWE_{max} in the latter period of study (Figure 9). Further, warmer winter temperatures from 1950 to 2009 (Thistle & Caissie, 2013; Zhang et al. 2011) increase winter runoff with earlier snow melting and decreasing spring snowpacks, thereby reducing peaks in spring runoff. The earlier spring freshet in some of the rivers in the latter half period can be attributed to warmer spring temperatures. These results on changing hydrological regimes in HB during the study period of 34 years are

similar with the findings of Déry et al.(2005) for HB, and Déry et al. (2009) for the rivers of western Canada.

6.4. Change in the Ratio of SWE_{max} to Runoff

The ratio of SWE_{max} to runoff quantifies the contribution of snow to the river discharge. The overall contribution of snow to HB river discharge for the study period of 34 years is 61.5% (see Table 10). This result is in agreement with the findings of Barnett et al. (2005). It shows that snow plays a critical role in governing the hydrological regime of the HB region, thus affecting the ecological and socio-economic characteristics across the region. The statistically significant decreasing trend of R_{SR} in HB rivers (Figure 16 and Figure 17) shows that the contribution of snow in the river discharge of HB is decreasing over the study period of 34 years. These results are similar to the findings of Kang et al. (2014) who explored at the changing contribution of snow to the hydrology of the Fraser River Basin, in British Columbia, Canada.

6.5. Limitations of Study

6.5.1 Selection of SWE Data

Some of the limitations of this study include the selection and use of the SWE data. After some investigation and preliminary analysis, GlobSnow SWE was considered to be the most appropriate dataset for this research, although some missing daily SWE data exist. The possibility of merging GlobSnow SWE data with another daily SWE data product, as a means of filling in missing gaps, was not attempted due to differences in their resolution and time constraints. A continuous daily SWE dataset would have improved the accuracy of SWE_{max}

estimation. In addition, use of continuous daily SWE data would improve the trend analysis of the timing of SWE_{max} that shows changing snow conditions over the HB region. Furthermore, the relatively coarse resolution of passive microwave remote sensing GlobSnow SWE data could limit the actual representation of the local snow conditions in a basin.

6.5.2 Validation of SWE Data

Validation of the SWE data is performed only with CMC SWE data because they are also available at essentially the same spatial resolution. The CMC SWE data are only available in monthly averages; therefore, this limits the validation of GlobSnow daily SWE_{max} data used for analysis in this study. It is difficult to compare point (observational) data with remote sensing data at a 25 km × 25 km scale; therefore the validation of GlobSnow SWE data using station data was not performed. Furthermore, the validation of GlobSnow SWE time series using independent reference data from Eurasia, Finland and Canada has been performed by Takala et al. (2011), showing its potential application for climatological analysis over North America.

6.5.3 Selection of River Basins

The availability of long term and continous hydrometric station data remains a challenge in this type of research. Furthermore, the changes in the hydrometric gauges in operation affects the availability of streamflow data for the study period (Mlynowski, Hernández-Henríquez, & Déry, 2011). Therefore, only 20 rivers in the HB watershed have been selected for this study based on long term and continous availability of streamflow data.

6.6. The Ecological and Social Implications of Snow and Streamflow Change in Hudson Bay

The ecological and social implications of observed changes in HB snow and streamflow are discussed based on some of the published literature.

6.6.1 Impacts to Polar Bears, Ringed Seals and Humans

Polar bears and seals are some of the native species of the HB region. Polar bears use Arctic sea ice to hunt and move between feeding and resting areas (Norris et al., 2002). Their primary prey are the ringed seals (*Phoca hispida*), but they also hunt bearded seals (*Erignathus barbatus*), harp seals (*Phoca groenlandica*), young walrus (*Odobenus rosmarus*), beluga whales (*Delphinapterus leucas*), narwhals (*Monodon monoceros*), fish, and seabirds and their eggs (Norris et al., 2002; Thiemann, Iverson, & Stirling, 2008). There are about 62,157±5,344 ringed seals found along all the coasts of JB and HB (DFO 2011). Similarly, the population of polar bears is estimated to be 711 in western HB (Atkinson et al., 2012). Further, polar bears are found along southern HB as well (Norris et al., 2002). However, between 1990 and 2010 studies find that the population of these species is declining in the HB region (Atkinson et al., 2012).

Regehr, Lunn, Amstrup, & Stirling (2007) found that the population of polar bears in western HB has declined from 1,194 in 1987 to 955 in 2004. During 1981 to 1998, Stirling, Lunn, & Iacozza (1999) also observed significant declines in the body condition and natality of male and female polar bears. Similarly, in the southern HB, a significant decline in the body mass of polar bears was detected by Obbard, McDonald, Howe, Regehr, & Richardson (2007) during 2003 to 2005 as compared to that of 1984 to 1986. Further, Ferguson, Stirling, & Mcloughlin (2005) found that the survival rates of ringed seals from fetuses to the age of harvest during 1999 to 2001 are decreasing as compared to that of 1991 to 1992 in western HB. Similarly, lower

pregnancy rates and reduced production of pups for ringed seals from the same area during 1991 to 2000 are reported by Stirling (2005). In addition, in a series of aerial surveys, Ferguson & Young (2011) found a declining trend in ringed seal density during 1995 to 2010 over western HB.

The prominent reason for such declining trends of these species and increased predation of seals from polar bears in HB is due to an earlier ice breakup during the 1990's and the first decade of the twenty-first century. Studies such as Dyck et al. (2007), Ferguson et al. (2005), Peacock, Derocher, Lunn, & Obbard (2010), Regehr et al. (2007), and Stirling et al. (1999) show that the earlier ice breakup has a direct impact on declining populations of these species. The interaction and relationship of sea ice and river discharge is a complex process; however, studies show that ablation of sea ice in estuaries and delta regions is enhanced by spring river discharge that delivers sensible heat accelerating ice melt in the nearshore region (Holt, Kelly, & Cherry, 1984; Kuzyk et al. 2008; Searcy, Dean, & Stringer, 1996). Therefore, the negative impact in the habitat of local species of the HB region and its influence on the local communities which depend on subsistence hunting may be related to the earlier runoff in the HB rivers.

Further, there are cases of high infection rates of Inuit by the parasite *toxoplasma gondii*, a zoonotic protozoan. The oocysts of the parasite are transported to HB via surface runoff, particularly during the spring snowmelt period. Lynx are the primary initial vectors for these parasites and the oocysts are shed out into the soil through their faeces. It then enters into the food chain via estuarine filter feeding molluscs and snails on which seals and other marine mammals may feed. This then infects the seals and by eating their raw meat, Inuit people as well (Simon, Bigras-Poulin, et al. 2013; Simon, Rousseau, et al. 2013). This suggests that continued

monitoring of snow accumulation and runoff into HB is of vital importance to human health and community well being.

6.6.2 Impacts on Hydroelectric Generation

The findings of this study reveal the changing conditions of snow and streamflow in the HB region. This impacts the hydropower generation in the region as it is influenced by regional water resources and is very sensitive to the changes in quantity and seasonality of runoff in a basin (Koch et al. 2011). There are many hydropower plants in the region operated by Manitoba Hydro, Ontario Power Generation and Hydro-Québec. Manitoba Hydro produces about 5,217 MW of hydroelectricity (Manitoba Hydro, 2015), Ontario Power Generation produces about 7,438 MW (Ontario Power Generation, 2015) and Hydro-Québec produces about 35,364 MW (Hydro-Québec, 2013) that is distributed in Canada and nearby states of the United States. The increasing winter runoff, earlier spring runoff and decreasing summer runoff would influence the efficiency of hydropower generation by affecting the reservoir capacities and operations of power plants. It further creates risks on the safety of existing dam structures, their design and their functioning due to change in runoff timing and magnitude (Prowse et al. 2009). Studies show that with the changing hydrological regime, there is a slight to severe decline in hydroelectric power generation in many basins of the world (Koch et al. 2011; Madani & Lund, 2010; Vicuna & Dracup, 2007).

7. Conclusions, Recommendations and Future Work

7.1. Conclusion

Snow plays an important role in the generation of streamflow globally. When precipitation is in the form of snow during winter, water is first stored in the snowpack, often for several months. The winter snowpack melts in the spring thereby contributing to runoff generation that serves as a major source of water for streamflow and groundwater recharge.

There are a number of studies showing changing snow and streamflow conditions in snow-dominated regions, influencing the timing and magnitude of runoff generation. Hudson Bay is the largest inland body of water of North America with a nival river regime that contributes a fifth of the total annual river discharge to the Arctic Ocean. HB has experienced changes in snow and streamflow conditions during the latter half of the 20th century and early 21st century. Such changes, in turn, have impacted the hydro-climatic, ecological, and socio-economic aspects of the region. It is, therefore, important to quantify the changing contribution of snow to streamflow generation.

7.1.1 Changing Snow Condition in Hudson Bay

Average annual SWE_{max} in the 20 watersheds of the Hudson Bay region is 126.3 mm over the study period of 1980 to 2013. The trend of the total annual SWE_{max} in HB is decreasing at the rate of 0.4 mm yr^{-1} (p <0.05). Annual maximum SWE_{max} in HB is 169.9 mm that occurred in 1997, and the total annual minimum SWE_{max} is 94.2 mm that occurred in 2010. The maximum SWE_{max} in 1997 is likely due to the frequent occurrence of snowstorms in winter of that year caused by the La Nina, while the minimum in 2010 may be associated with an El Niño event

causing less snowfall. For the entire HB region, SWE_{max} has decreased by 15.3 mm $(34\ yr)^{-1}$ and by 2013 it has decreased by 11.7 % from its value in 1980. Out of the 20 watersheds, 18 show a decreasing trend of the annual SWE_{max} with 10 of them being statistically significant.

The eastern Hudson Bay comprising nine river basins has a mean annual SWE_{max} of 178.5 mm whereas western HB with 11 river basins has a mean annual SWE_{max} of 118.1 mm over a period of 34 years. The higher mean annual SWE_{max} in the eastern side of HB is likely because the mean annual total precipitation and maximum snow depth is higher than in the western part of the basin. The total SWE_{max} in the eastern and western parts of HB has decreased by 37.4 mm $(34\ yr)^{-1}$ and 10.2 mm $(34\ yr)^{-1}$, respectively. By 2013, the total annual SWE_{max} in eastern and western HB has decreased by 26.5% and 8.3% from its value in 1980. Both of them show similar patterns in annual SWE_{max} with maximum values in 1997 and minimum values in 2010.

Over a period of 34 years, the regulated basins (with SWE_{max} from five basins) have a mean annual SWE_{max} of 111.8 mm with a decreasing trend of 37.4 mm $(34\ yr)^{-1}$. The unregulated basins (SWE_{max} from 15 basins) have a mean SWE_{max} of 152.1 mm with a statistically significant decreasing trend of 27.2 mm $(34\ yr)^{-1}$. By 2013, the total annual SWE_{max} in regulated and unregulated basins of HB has decreased by 33.6% and 18.1%, respectively from its value in 1980. Both of them show similar patterns in annual SWE_{max} with maximum and minimum values in 1997 and 2010, respectively.

7.1.2 Changing Runoff Condition in Hudson Bay

Average annual runoff in the 20 watersheds of the Hudson Bay region is 206.2 mm over the study period of 1980 to 2013. The trend of the total annual runoff in HB is increasing at the rate

of 1.0 mm yr^{-1} yr^{-1}. Annual maximum runoff in HB of 244.6 mm occurred in 2005, and the total annual minimum runoff of 173.5 mm occurred in 1982. The maximum runoff in 2005 is likely due to flooding caused by higher precipitation in the Nelson River Basin. In addition, the minimum runoff in 1982 may be attributed to reduced inflow into HB due to higher rates of evapotranspiration the basin. For the entire HB region, runoff has increased by 34.3 mm $(34\ yr)^{-1}$ and, by 2013, had risen 17.4% from its value in 1980. Out of the 20 watersheds, 13 show an increasing trend of the annual runoff with four of them being statistically significant.

Eastern Hudson Bay comprising runoff from nine river basins has a mean annual runoff of 565.1 mm and the western HB with runoff from 11 river basins has a mean annual runoff of 143.9 mm over the period of 34 years. The higher mean annual runoff on the eastern side of HB than on the western side is likely due to the annual mean total precipitation and maximum snow depth in the eastern part of HB is higher than in the western part. The total runoff in the eastern and western parts of HB shows a statistically significant increasing trend of 1.2 mm yr^{-1} yr^{-1} and 1.0 mm yr^{-1} yr^{-1} respectively ($p<0.05$). By 2013, the total annual runoff in eastern and western HB has increased by 6.8% and 26.9% from its value in 1980.

Over a period of 34 years, the regulated basins (five basins) and unregulated basins (15 basins) have a mean annual runoff of 156.5 mm and 296.6 mm, respectively. The mean annual runoff in regulated basins is increasing with a statistically significant increasing trend of 1.3 mm yr^{-1} yr^{-1} and unregulated basins show relatively lower increasing trend of 0.4 mm yr^{-1} yr^{-1}. By 2013, the total annual runoff in regulated and unregulated basins of HB has increased by 30.1% and 4.8%, respectively from its value in 1980. Both of them show similar patterns in annual runoff with maximum values during 2005 to 2006.

Trends in daily runoff show a change in intensity throughout the hydrological year. For some of the rivers, a prominent shift to earlier timing of the spring freshet is observed in between the last week of April and the third week of June. Further an increasing trend in winter runoff is observed. This may be attributed to more likelihood of rain than snow, earlier snowmelt, and reduced SWE accumulation combined with the warming spring air temperature recorded in the latter part of the 20th century and early 21st century.

While comparing the mean annual cycle of daily runoff in the unregulated Hudson Bay rivers for 1980 to 1996 and 1997 to 2013, high magnitude of runoff in spring is observed in the first half of the study period for 11 rivers out of 14 studied rivers. This is likely caused by reduced SWE accumulation in the latter period compared to first half of the study period. Relatively high runoff during the first three months of a hydrological year from October to December in nine of the 14 rivers observed in latter half study period may be attributed to runoff generated by precipitation in the form of rain during the winter.

7.1.3 Changing R_{SR} Condition in Hudson Bay

The ratio of SWE_{max} to runoff in Hudson Bay rivers is decreasing. Out of the 20 rivers, 19 show a decreasing trend of the annual R_{SR} with nine of them being statistically significant. The total annual R_{SR} value of HB has decreased by 15.9% $(34\ yr)^{-1}$. The total annual maximum R_{SR} in HB of 0.8 occurred in 1987, and the total annual minimum R_{SR} of 0.4 occurred in 2008. In eastern and western HB, R_{SR} decreases by 10.2 % $(34\ yr)^{-1}$ and 27.2% $(34\ yr)^{-1}$ respectively. In regulated an unregulated basins of HB, R_{SR} decreases by 20.4 % $(34\ yr)^{-1}$ and 10.2% $(34\ yr)^{-1}$, respectively.

Overall during the study period of 34 years, the contribution of snow to runoff generation in 20 Hudson Bay rivers is 61.5% and it has decreased by 20.6% from its value in 1980. Such statistically significant decreasing trends of R_{SR} in HB rivers reveal the decreasing contribution of snow to the river discharge of HB over the study period of 34 years. This may be attributed to the decreasing SWE accumulation combined with warming air temperatures of the region.

7.1.4 Implications of the Results

The changing hydrological regime of the Hudson Bay drainage basin revealed in this study could contribute to the declining populations of its keystone species,: seals and polar bears. The sea ice breakage is accelerated by earlier spring runoff and increased winter runoff that impacts the habitat of seals and polar bears. Further, the study on impact of runoff change and effect of changes in regulated flows in HB sea-ice breakup would help to understand the reason of declining population of keystone species. The earlier freshet and runoff in winter found in this study reveals the possibility of accumulation of the parasite *toxoplasma gondii* in the region infecting the community. Further, the obtained result on the long term SWEmax, runoff and contribution of snow to runoff in the HB region can be useful to water resources authorities in making effective water operating policies for dam construction, reservoir flow regulation, water allocation for agricultural purposes, scheduling hydropower generation and other applications (Sarhadi, Kelly, & Modarres, 2014).

7.2. Recommendations and Future Work

To obtain more accurate SWE_{max}, use of finer resolution SWE data would be helpful in improving results. Further, use of a high resolution model that produces simulated SWE and runoff would give results in a finer spatial scale and larger basin area of HB could be covered in the study. In addition, the modelled data can be used for future simulations to assess the hydrologic response of SWE, runoff and their ratios under different scenarios. Use of continuous daily SWE data is recommended to improve calculations of SWE_{max}. Merging of GlobSnow SWE data with any other available daily SWE data product would help to fill the missing gaps in GlobSnow SWE data and to enhance the analysis of SWE_{max}. The establishment and operation of more weather and snow pillow stations in and around HB would help in monitoring snow conditions of the region more precisely and provide valuable *in situ* data to validate remote sensing products.

Inclusion of streamflow data from more rivers of HB would give better information on changing streamflow conditions over the HB region. Further, obtaining SWE_{max} for more basins and looking over R_{SR} at larger spatial scales would provide better results on the overall contribution of snow to HB river discharge. Extracting the streamflow data using a high resolution hydrologic model over HB would provide better temporal and spatial estimation of streamflow over the entire region. Further, obtaining SWE data along with streamflow data from the same hydrologic model would provide an opportunity to estimate the contribution of snow in runoff generation at a grid scale.

The study on hydrologic responses of SWE_{max}, runoff and R_{SR} with respect to the changing air temperature and precipitation would be useful to observe the possible impact of climate change on the hydrology of the Hudson Bay. This would aid to estimate the response of these hydrologic

variables over the changing climatic conditions. Further, it helps to foresee the changing contribution of snow on river discharge for different climatic scenarios. This research and future research in this area could benefit communities along the watersheds of HB by informing about the changing streamflow condition and predicting flooding. Further, providing information on sea ice conditions would be important especially for hunters.

References

Abdi, H. (2010). Coefficient of variation. *Encyclopedia of Research Design*, 1–5.

Adam, J. C., Hamlet, A. F., & Lettenmaier, D. P. (2009). Implications of global climate change for snowmelt hydrology in the twenty-first century. *Hydrological Processes*, *23*, 962–972. http://doi.org/10.1002/hyp

Armstrong, R. L., & Brun, E. R. (2008). *Snow and climate*. Cambridge University Press.

Arora, V. K., & Boer, G. J. (2001). Effects of simulated climate change on the hydrology of major river basins. *Journal of Geophysical Research*, *106*, 3335–3348. http://doi.org/10.1029/2000JD900620

Atkinson, S., Garshelis, D., Stapleton, S., & Hedman, D. (2012). *Western Hudson Bay polar bear aerial survey. Government of Nunavut, Department of Environment.*

Barnett, T. P., Adam, J. C., & Lettenmaier, D. P. (2005). Potential impacts of a warming climate on water availability in snow-dominated regions. *Nature*, *438*(17), 303–309. http://doi.org/10.1038/nature04141

Berkes, F., & Freeman, M. M. R. (1986). Human ecology and resource use. In I. P. Martini (Ed.), *Canadian Inland Seas* (pp. 425–455). Elsevier Science Publishes B.V.

Brown, R. D. (2000). Northern Hemisphere snow cover variability and change, 1915-97. *Journal of Climate*, *13*, 2339–2355.

Brown, R. D., & Braaten, R. O. (1998). Spatial and temporal variability of Canadian monthly snow depths, 1946-1995. *Atmosphere-Ocean*, *36*(1), 37–54. http://doi.org/10.1080/07055900.1998.9649605

Brown, R. D., & Brasnett, B. (2013). Canadian Meteorological Centre (CMC) Daily Snow Depth Analysis Data. Boulder, Colorado USA: NASA DAAC at the National Snow and Ice Data Center. Retrieved from http://nsidc.org/data/docs/daac/nsidc0447_CMC_snow_depth/index.html

Brown, R. D., & Mote, P. W. (2009). The response of Northern Hemisphere snow cover to a changing climate. *Journal of Climate*, *22*, 2124–2145. http://doi.org/10.1175/2008JCLI2665.1

Brown, R. D., & Robinson, D. A. (2011). Northern Hemisphere spring snow cover variability and change over 1922-2010 including an assessment of uncertainty. *Cryosphere*, *5*(2000), 219–229. http://doi.org/10.5194/tc-5-219-2011

Buttle, J. M., Boon, S., Peters, D. L., Spence, C., van Meerveld, H. J., & Whitfield, P. H. (2012). An overview of temporary stream hydrology in Canada. *Canadian Water Resources Journal*, *37*(4), 279–310. http://doi.org/10.4296/cwrj2011-903

Choi, G., Robinson, D. A., & Kang, S. (2010). Changing Northern Hemisphere snow seasons. *Journal of Climate*, *23*, 5305–5310. http://doi.org/10.1175/2010JCLI3644.1

Derksen, C., & Brown, R. (2012). Spring snow cover extent reductions in the 2008-2012 period exceeding climate model projections. *Geophysical Research Letters*, *39*(19), L19504.

http://doi.org/10.1029/2012GL053387

Derksen, C., & MacKay, M. (2006). The Canadian boreal snow water equivalent band. *Atmosphere-Ocean*, *44*(3), 305–320. http://doi.org/10.3137/ao.440307

Déry, S. J., & Brown, R. D. (2007). Recent Northern Hemisphere snow cover extent trends and implications for the snow-albedo feedback. *Geophysical Research Letters*, *34*(22), L22504. http://doi.org/10.1029/2007GL031474

Déry, S. J., Hernández-Henríquez, M. A., Burford, J. E., & Wood, E. F. (2009). Observational evidence of an intensifying hydrological cycle in northern Canada. *Geophysical Research Letters*, *36*, L13402. http://doi.org/10.1029/2009GL038852

Déry, S. J., Mlynowski, T. J., Hernández-Henríquez, M. A., & Straneo, F. (2011). Interannual variability and interdecadal trends in Hudson Bay streamflow. *Journal of Marine Systems*, *88*, 341–351. http://doi.org/10.1016/j.jmarsys.2010.12.002

Déry, S. J., Sheffield, J., & Wood, E. F. (2005). Connectivity between Eurasian snow cover extent and Canadian snow water equivalent and river discharge. *Journal of Geophysical Research:Atmosphere*, *110*, D23106. http://doi.org/10.1029/2005JD006173

Déry, S. J., Stahl, K., Moore, R. D., Whitfield, P. H., Menounos, B., & Burford, J. E. (2009). Detection of runoff timing changes in pluvial, nival, and glacial rivers of western Canada. *Water Resources Research*, *45*, W04426. http://doi.org/10.1029/2008WR006975

Déry, S. J., Stieglitz, M., Mckenna, E. C., & Wood, E. F. (2005). Characteristics and trends of river discharge into Hudson, James, and Ungava Bays, 1964-2000. *Journal of Climate*, *18*, 2540–2557.

Déry, S. J., & Wood, E. F. (2004). Teleconnection between the Arctic Oscillation and Hudson Bay river discharge. *Geophysical Research Letters*, *31*(18), L18205. http://doi.org/10.1029/2004GL020729

Déry, S. J., & Wood, E. F. (2005). Decreasing river discharge in northern Canada. *Geophysical Research Letters*, *32*(10), L10401. http://doi.org/10.1029/2005GL022845

DeWalle, D. R., & Rango, A. (2008). *Principles of snow hydrology*. Cambridge University Press.

DFO. (2009). *Review of aerial survey estimates for ringed seals (Phoca hispida) in western Hudson Bay. DFO Can. Sci. Advis. Sec. Sci. Advis. Rep. 2009/004.*

DFO. (2011). *Review of aerial survey estimates for ringed seals (Phoca hispida) in western Hudson Bay, 2009 and 2010. DFO Can. Sci. Advis. Sec. Sci. Advis. Rep. 2011/024.* Retrieved from http://www.dfo-mpo.gc.ca/Library/336456.pdf

Dyck, M. G., Soon, W., Baydack, R. K., Legates, D. R., Baliunas, S., Ball, T. F., & Hancock, L. O. (2007). Polar bears of western Hudson Bay and climate change: Are warming spring air temperatures the "ultimate" survival control factor? *Ecological Complexity*, *4*, 73–84. http://doi.org/10.1016/j.ecocom.2007.03.002

Dyer, J. (2008). Snow depth and streamflow relationships in large North American watersheds. *Journal of Geophysical Research*, *113*, D18113. http://doi.org/10.1029/2008JD010031

Dyer, J. L., & Mote, T. L. (2007). Trends in snow ablation over North America. *International*

Journal of Climatology, *27*, 739–748. http://doi.org/10.1002/joc

ESRI. (2011). ArcGIS Desktop: Release 10. Redlands, CA: Environmental Systems Research Institute.

Etkin, D. A. (1991). Break-up in Hudson Bay : its sensitivity to air temperatures and implications for climate warming. *Climatological Bulletin*, *25*(1), 21–34.

Ferguson, S. H., Stirling, I., & McLoughlin, P. (2005). Climate change and ringed seal (Phoca hispida) recruitment in western Hudson Bay. *Marine Mammal Science*, *21*(1), 121–135.

Ferguson, S. H., & Young, B. G. (2011). Aerial survey estimates of hauled-out Ringed Seal (Phoca hispida) density in western Hudson Bay, June 2009 and 2010. *DFO Can. Sci. Advis. Sec. Res. Doc. 2011/029. Iv + 12 P.*

Flesch, T. K., & Reuter, G. W. (2012). WRF model simulation of two Alberta flooding events and the impact of topography. *Journal of Hydrometeorology*, *13*, 695–708. http://doi.org/10.1175/JHM-D-11-035.1

Gagnon, A. S., & Gough, W. A. (2002). Hydro-Climatic trends in the Hudson Bay region, Canada. *Canadian Water Resources Journal*, *27*(3), 245–262. http://doi.org/10.4296/cwrj2703245

Gagnon, A. S., & Gough, W. A. (2005a). Climate change scenarios for the Hudson Bay region: an intermodel comparison. *Climatic Change*, *69*, 269–297.

Gagnon, A. S., & Gough, W. A. (2005b). Trends in the dates of ice freeze-up and breakup over Hudson Bay, Canada. *Arctic*, *58*(4), 370–382.

Groisman, P. Y., Knight, R. W., Karl, T. R., Easterling, D. R., Sun, B., & Lawrimore, J. H. (2004). Contemporary changes of the hydrological cycle over the contiguous United States : Trends derived from in situ observations. *Journal of Hydrometeorology*, *5*, 64–85.

Hartmann, D. L., Tank, A. M. G. K., Rusticucci, M., Alexander, L. V., Brönnimann, S., Charabi, Y., … Zhai, P. M. (2013). Observations: Atmosphere and Surface. In T. F. Stocker, D. Qin, G.-K. Plattner, M. Tignor, S. K. Allen, J. Boschung, … P. M. Midgley (Eds.), *In: Climate Change 2013: The Physical Science Basis. Contribution of Working Group I to the Fifth Assessment Report of the Intergovernmental Panel on Climate Change*. Cambridge University Press, Cambridge, United Kingdom and New York, NY, USA.

Hernández-Henríquez, M. A., Mlynowski, T. J., & Déry, S. J. (2010). Reconstructing the natural streamflow of a regulated river: A case study of La Grande Rivière, Québec, Canada. *Canadian Water Resources Journal*, *35*(3), 301–316. http://doi.org/10.4296/cwrj3503301

Hidalgo, H. G., Das, T., Dettinger, M. D., Cayan, D. R., Pierce, D. W., Barnett, T. P., … Nozawa, T. (2009). Detection and attribution of streamflow timing changes to climate change in the western United States. *Journal of Climate*, *22*(13), 3838–3855. http://doi.org/10.1175/2009JCLI2470.1

Hochheim, K. P., Lukovich, J. V., & Barber, D. G. (2011). Atmospheric forcing of sea ice in Hudson Bay during the spring period, 1980-2005. *Journal of Marine Systems*, *88*, 476–487. http://doi.org/10.1016/j.jmarsys.2011.05.003

Hodgkins, G. A., & Dudley, R. W. (2006). Changes in the timing of winter-spring streamflows in eastern North America, 1913-2002. *Geophysical Research Letters*, *33*, L06402. http://doi.org/10.1029/2005GL025593

Hodgkins, G. A., Dudley, R. W., & Huntington, T. G. (2003). Changes in the timing of high river flows in New England over the 20th Century. *Journal of Hydrology*, *278*, 244–252. http://doi.org/10.1016/S0022-1694(03)00155-0

Holt, H., Kelly, P. M., & Cherry, B. S. G. (1984). Cryospheric impacts of soviet river. *Annals of Glaciology 5*, 61–68.

Hydro-Quebec. (2013). *Annual Report 2013*. Retrieved from http://reports.barclays.com/ar13/

Kang, D. H., Shi, X., Gao, H., & Déry, S. J. (2014). On the changing contribution of snow to the hydrology of the Fraser River Basin, Canada. *Journal of Hydrometeorology*, *15*, 1344–1365. http://doi.org/10.1175/JHM-D-13-0120.1

Kendall, M. G. (1970). *Rank Correlation Methods.* (4th ed.). Griffin.

Koch, F., Prasch, M., Bach, H., Mauser, W., Appel, F., & Weber, M. (2011). How will hydroelectric power generation develop under climate change scenarios? A case study in the Upper Danube Basin. *Energies*, *4*, 1508–1541. http://doi.org/10.3390/en4101508

Kokkonen, T., Koivusalo, H., Jakeman, A., & Norton, J. (2006). Construction of a degree-day snow model in the light of the ten iterative steps in model development. *Proceedings of the iEMSs Third Biennial Meeting: "Summit on Environmental Modelling and Software" (July 2006)*, (Step 2), 12. Retrieved from http://www.iemss.org/iemss2006/papers/w4/Kokkonen.pdf

Kuzyk, Z. A., Macdonald, R. W., Granskog, M. A., Scharien, R. K., Galley, R. J., Michel, C., … Stern, G. (2008). Sea ice, hydrological, and biological processes in the Churchill River estuary region, Hudson Bay. *Estuarine, Coastal and Shelf Science*, *77*, 369–384. http://doi.org/10.1016/j.ecss.2007.09.030

Labat, D., Goddéris, Y., Probst, J. L., & Guyot, J. L. (2004). Evidence of global runoff increase releated to climate warming. *Advances in Water Resources*, *27*, 631–642. http://doi.org/10.1016/j.advwatres.2004.02.020

Lammers, R. B., Shiklomanov, A. I., Vörösmarty, C. J., Fekete, B. M., & Peterson, B. J. (2001). Assessment of contemporary Arctic river runoff based on observational discharge records. *Journal of Geophysical Research*, *106*(D4), 3321–3334. http://doi.org/10.1029/2000JD900444

LeBlond, P. H., Lazier, J. R., & Weaver, A. J. (1996). Can regulation of freshwater runoff in Hudson Bay affect the climate of the north Atlantic? *Arctic*, *49*(4), 348–355.

Li, Z., Liu, J., Huang, L., Wang, N., Tian, B., Zhou, J., … Zhang, P. (2014). Snow mass decrease in the Northern Hemisphere (1979/80-2010/11). *The Cryosphere Discussions*, *8*, 1–19. http://doi.org/10.5194/tcd-8-1-2014

Liston, G. E., & Hiemstra, C. A. (2011). The changing cryosphere: Pan-Arctic snow trends (1979-2009). *Journal of Climate*, *24*, 5691–5712. http://doi.org/10.1175/JCLI-D-11-00081.1

Liu, J., Li, Z., Huang, L., & Tian, B. (2014). Hemispheric-scale comparison of monthly passive microwave snow water equivalent products. *Journal of Applied Remote Sensing*, *8*(1), 084688. http://doi.org/10.1117/1.JRS.8.084688

Lunn, N. J., Stirling, I., & Nowicki, S. N. (1997). Distribution and abundance of ringed (Phoca hispida) and bearded seals (Erignathus barbatus) in western Hudson Bay. *Canadian Journal of Fisheries and Aquatic Sciences*, *54*, 914–921. http://doi.org/10.1139/f96-346

Luojus, K., Pulliainen, J., Takala, M., Derksen, C., Rott, H., Nagler, T., … Bojkov, B. (2010). Investigating the feasibility of the globsnow snow water equivalent data for climate research purposes. In *Geoscience and Remote Sensing Symposium (IGARSS), 2010 IEEE International* (Vol. 19, pp. 4851–4853). IEEE,2010. http://doi.org/10.1109/IGARSS.2010.5741987

Luojus, K., Pulliainen, J., Takala, M., Kangwa, M., Smolander, T., Wiesmann, A., … Husler, F. (2013). GlobSnow-2 Product User Guide Version 1.0.

Macdonald, R. W., & Kuzyk, Z. Z. A. (2011). The Hudson Bay system: A northern inland sea in transition. *Journal of Marine Systems*, *88*, 337–340. http://doi.org/10.1016/j.jmarsys.2011.06.003

Manitoba Hydro. (2015). Generating stations. Retrieved September 16, 2015, from https://www.hydro.mb.ca/corporate/facilities/generating_stations.shtml

Mann, H. B. (1945). Nonparametric tests against trend. *Econometrica*, *13*, 245–259.

Maurer, E. P., Stewart, I. T., Bonfils, C., Duffy, P. B., & Cayan, D. (2007). Detection, attribution, and sensitivity of trends toward earlier streamflow in the Sierra Nevada. *Journal of Geophysical Research*, *112*, D11118. http://doi.org/10.1029/2006JD008088

McClelland, J. W., Déry, S. J., Peterson, B. J., Holmes, R. M., & Wood, E. F. (2006). A pan-arctic evaluation of changes in river discharge during the latter half of the 20th century. *Geophysical Research Letters*, *33*(6), L06715. http://doi.org/10.1029/2006GL025753

McCuen, R. H. (2003). *Modeling Hydrologic Change: Statistical Methods*. Lewis Publishers.

McNamara, J. P., Kane, D. L., & Hinzman, L. D. (1998). An analysis of streamflow hydrology in the Kuparuk River Basin, Arctic Alaska: A nested watershed approach. *Journal of Hydrology*, *206*, 39–57. http://doi.org/10.1016/S0022-1694(98)00083-3

Mekis, É., & Vincent, L. A. (2011). An overview of the second generation adjusted daily precipitation dataset for trend analysis in Canada. *Atmosphere-Ocean*, *49*(2), 163–177. http://doi.org/10.1080/07055900.2011.583910

Minville, M., Brissette, F., Krau, S., & Leconte, R. (2009). Adaptation to climate change in the management of a Canadian water-resources system exploited for hydropower. *Water Resources Management*, *23*, 2965–2986. http://doi.org/10.1007/s11269-009-9418-1

Mlynowski, T. J., Hernández-Henríquez, M. A., & Déry, S. J. (2011). An evaluation of hydrometric monitoring across the Canadian pan-Arctic region, 1950-2008. *Hydrology Research*, *42*(6), 479. http://doi.org/10.2166/nh.2011.105

Moore, J. N., Harper, J. T., & Greenwood, M. C. (2007). Significance of trends toward earlier

snowmelt runoff, Columbia and Missouri Basin headwaters, western United States. *Geophysical Research Letters*, *34*, L16402. http://doi.org/10.1029/2007GL031022

Mote, P. W., Hamlet, A. F., Clark, M. P., & Lettenmaier, D. P. (2005). Declining mountain snowpack in Western North America. *Bulletin of the American Meteorological Society*, *86*, 39–49. http://doi.org/10.1175/BAMS-86-1-39

Nash, J. E., & Sutcliffe, J. V. (1970). River flow forecasting through conceptual models part I-A discussion of principles. *Journal of Hydrology*, *10*. http://doi.org/10.1016/0022-1694(70)90255-6

Natural Resources Canada. (2009). The Atlas of Canada. Retrieved January 4, 2016, from http://www.nrcan.gc.ca/earth-sciences/geography/atlas-canada/selected-thematic-maps/16888

Newbury, R. W., McCullough, G. K., & Hecky, R. E. (1984). The Southern Indian lake impoundment and Churchill River diversion. *Canadian Journal of Fish and Aquatic Science*, *41*, 548–557.

Norris, S., Rosentrater, L., & Eid, P. M. (2002). *Polar bears at risk. WWF International Arctic Programme*. Oslo Norway. Retrieved from http://www.panda.org/about_wwf/where_we_work/arctic/index.cfm

Obbard, M. E., McDonald, T. L., Howe, E. J., Regehr, E. V., & Richardson, E. S. (2007). *Polar bear population status in Southern Hudson Bay, Canada. USGS Science Strategy to Support U.S. Fish and Wildlife Service Polar Bear Listing Decision.*

Ogi, M., Tachibana, Y., Nishio, F., & Danchenkov, M. A. (2001). Does the Fresh Water Supply from the Amur River Flowing into the Sea of Okhotsk Affect Sea Ice Formation? *Journal of the Meteorological Society of Japan*, *79*(1), 123–129. http://doi.org/10.2151/jmsj.79.123

Ontario Power Generation. (2015). Ontario Power Generation. Retrieved from http://www.opg.com/index.asp

Park, H., Yabuki, H., & Ohata, T. (2012). Analysis of satellite and model datasets for variability and trends in Arctic snow extent and depth, 1948-2006. *Polar Science*, *6*, 23–37. http://doi.org/10.1016/j.polar.2011.11.002

Peacock, E., Derocher, A. E., Lunn, N. J., & Obbard, M. E. (2010). Polar bear ecology and management in Hudson Bay in the face of climate change. In S. H. Ferguson, L. L. Loseto, & M. L. Mallory (Eds.), *A Little Less Arctic* (pp. 93–116). Springer Netherlands. http://doi.org/10.1007/978-90-481-9121-5

Prinsenberg, S. J. (1988). Ice-cover and ice-ridge contributions to the freshwater contents of Hudson Bay and Foxe Basin. *Arctic*, *41*(1), 6–11.

Prowse, T. D., Furgal, C., Chouinard, R., Melling, H., Milburn, D., & Smith, S. L. (2009). Implications of climate change for economic development in northern Canada: energy, resource, and transportation sectors. *A Journal of the Human Environment*, *38*(5), 272–281. http://doi.org/10.1579/0044-7447-38.5.272

Pulliainen, J. (2006). Mapping of snow water equivalent and snow depth in boreal and sub-arctic zones by assimilating space-borne microwave radiometer data and ground-based

observations. *Remote Sensing of Environment*, *101*(2), 257–269. http://doi.org/10.1016/j.rse.2006.01.002

R Development Core Team. (2011). R: A Language and Environment for Statistical Computing. Vienna, Austria : the R Foundation for Statistical Computing. Retrieved from http://www.r-project.org/.

Rasouli, K., Hernández-Henríquez, M. A., & Déry, S. J. (2013). Streamflow input to Lake Athabasca, Canada. *Hydrology and Earth System Sciences*, *17*, 1681–1691. http://doi.org/10.5194/hess-17-1681-2013

Regehr, E. V., Lunn, N. J., Amstrup, S. C., & Stirling, I. (2007). Effects of earlier sea ice breakup on survival and population size of polar bears in Western Hudson Bay. *Journal of Wildlife Management*, *71*(8), 2673–2683. http://doi.org/10.2193/2006-180

Rennermalm, A. K., Wood, E. F., Weaver, A. J., Eby, M., & Déry, S. J. (2007). Relative sensitivity of the Atlantic meridional overturning circulation to river discharge into Hudson Bay and the Arctic Ocean. *Journal of Geophysical Research: Biogeosciences*, *112*(4), 1–12. http://doi.org/10.1029/2006JG000330

Rodgers, J. L., & Nicewander, W. A. (1988). Thirteen Ways to Look at the Correlation Coefficient. *The American Statistician*, *42*(1), 59–66.

Rood, S. B., Pan, J., Gill, K. M., Franks, C. G., Samuelson, G. M., & Shepherd, A. (2008). Declining summer flows of Rocky Mountain rivers: Changing seasonal hydrology and probable impacts on floodplain forests. *Journal of Hydrology*, *349*, 397–410. http://doi.org/10.1016/j.jhydrol.2007.11.012

Rosenberg, D. M., Chambers, P. A., Culp, J. M., Franzin, W. G., Nelson, P. A., Salki, A. G., … Newbury, R. W. (2005). Chapter 19: Nelson and Churchill River Basins. In A. C. Benke & C. E. Cushing (Eds.), *Rivers of North America* (pp. 853–901). Elsevier Academic Press, Oxford.

Sarhadi, A., Kelly, R., & Modarres, R. (2014). Snow water equivalent time-series forecasting in Ontario, Canada, in link to large atmospheric circulations. *Hydrological Processes*, *28*, 4640–4653. http://doi.org/10.1002/hyp.10184

Saucier, F. J., Senneville, S., Prinsenberg, S., Roy, F., Smith, G., Gachon, P., … Laprise, R. (2004). Modelling the sea ice-ocean seasonal cycle in Hudson Bay, Foxe Basin and Hudson Strait, Canada. *Climate Dynamics*, *23*(3-4), 303–326. http://doi.org/10.1007/s00382-004-0445-6

Sen, P. K. (1968). Estimates of the regression coefficient based on Kendall's Tau. *Journal of the American Statistical Association*, *63*(324), 1379–1389.

Serreze, M. C., Bromwich, D. H., Clark, M. P., Etringer, A. J., Zhang, T., & Lammers, R. (2003). Large-scale hydro-climatology of the terrestrial Arctic drainage system. *Journal of Geophysical Research*, *108*, D28160. http://doi.org/10.1029/2001JD000919

Shabbar, A., & Khandekar, M. (1996). The impact of El Nino-Southern Oscillation on the temperature field over Canada: Research note. *Atmosphere-Ocean*, *34*(2), 401–416. http://doi.org/10.1080/07055900.1996.9649570

Shein, K. A. (2006). State of the climate in 2005. *Bulletin of the American Meteorological Society*, *87*(6), s1–s102.

Shi, X., Déry, S. J., Groisman, P. Y., & Lettenmaier, D. P. (2013). Relationships between recent pan-Arctic snow cover and hydroclimate trends. *Journal of Climate*, *26*(6), 2048–2064. http://doi.org/10.1175/JCLI-D-12-00044.1

Shiklomanov, A. I., Yakovleva, T. I., Lammers, R. B., Karasev, I. P., Vörösmarty, C. J., & Linder, E. (2006). Cold region river discharge uncertainty-estimates from large Russian rivers. *Journal of Hydrology*, *326*, 231–256. http://doi.org/10.1016/j.jhydrol.2005.10.037

Shiklomanov, I. A., & Shiklomanov, A. I. (2003). Climatic Change and the dynamics of river runoff into the Arctic Ocean. *Water Resources*, *30*(6), 593–601. http://doi.org/10.1023/B:WARE.0000007584.73692.ca

Simon, A., Bigras-Poulin, M., Rousseau, A. N., & Ogden, N. H. (2013). Fate and transport of Toxoplasma gondii oocysts in seasonally snow covered watersheds: a conceptual framework from a melting snowpack to the Canadian Arctic coasts. *International Journal of Environmental Research and Public Health*, *10*, 994–1005. http://doi.org/10.3390/ijerph10030994

Simon, A., Rousseau, A. N., Savary, S., Bigras-Poulin, M., & Ogden, N. H. (2013). Hydrological modelling of Toxoplasma gondii oocysts transport to investigate contaminated snowmelt runoff as a potential source of infection for marine mammals in the Canadian Arctic. *Journal of Environmental Management*, *127*, 150–161. http://doi.org/10.1016/j.jenvman.2013.04.031

Smith, T. G. (1975). Ringed seals in James Bay and Hudson Bay: Population estimates and catch statistics. *Arctic*, *28*(3), 170–182.

Statistics Canada. (2013). Aboriginal Population Profile, 2011. Retrieved March 9, 2016, from http://www12.statcan.gc.ca/nhs-enm/2011/dp-pd/aprof/index.cfm?Lang=E

Stewart, I. T. (2009). Changes in snowpack and snowmelt runoff for key mountain regions. *Hydrological Processes*, *23*, 78–94. http://doi.org/10.1002/hyp

Stewart, I. T., Cayan, D. R., & Dettinger, M. D. (2005). Changes toward earlier streamflow timing across Western North America. *Journal of Climate*, *18*, 1136–1155.

Stirling, I. (2005). Reproductive rates of ringed seals and survival of pups in Northwestern Hudson Bay, Canada, 1991-2000. *Polar Biology*, *28*, 381–387. http://doi.org/10.1007/s00300-004-0700-7

Stirling, I., Lunn, M. J., & Iacozza, J. (1999). Long-term trends in the population ecology of polar bears in Western Hudson Bay in relation to climate change. *Arctic*, *52*(3), 294–306. http://doi.org/10.14430/arctic935

Sturm, M., Holmgren, J., & Liston, G. E. (1995). A seasonal snow cover classification system for local to global applications. *Journal of Climate*, *8*, 1261–1283.

Sturm, M., Taras, B., Liston, G. E., Derksen, C., Jonas, T., & Lea, J. (2010). Estimating snow water equivalent using snow depth data and climate classes. *Journal of Hydrometeorology*, *11*(6), 1380–1394. http://doi.org/10.1175/2010JHM1202.1

Takala, M., Luojus, K., Pulliainen, J., Derksen, C., Lemmetyinen, J., Kärnä, J. P., … Bojkov, B. (2011). Estimating northern hemisphere snow water equivalent for climate research through assimilation of space-borne radiometer data and ground-based measurements. *Remote Sensing of Environment*, *115*, 3517–3529. http://doi.org/10.1016/j.rse.2011.08.014

Tam, B. Y., Gough, W. A. ., Edwards, V., & Tsuji, L. J. . (2013). The impact of climate change on the well-being and lifestyle of a First Nation community in the western James Bay region. *Canadian Geographer*, *57*(4), 441–456. http://doi.org/10.1111/j.1541-0064.2013.12033.x

Thiemann, G. W., Iverson, S. J., & Stirling, I. (2008). Polar bear diets and Arctic marine food webs : Insights from fatty acid analysis. *Ecological Monographs*, *78*(4), 591–613. Retrieved from http://www.jstor.org/stable/27646156

Thistle, M. E., & Caissie, D. (2013). Trends in air temperature, total precipitation, and streamflow characteristics in eastern Canada. In *Can. Tech. Rep. Fish. Aquat. Sci. 3018: xi + 97p.*

Thompson, D. W. J., & Wallace, J. M. (1998). The Arctic Oscillation signature in the wintertime geopotential height and temperature fields. *Geophysical Research Letters*, *25*(9), 1297–1300.

Trenberth, K. E., Jones, P. D., Ambenje, P., Bojariu, R., Easterling, D., Tank, A. K., … Zhai, P. (2007). Observations: Surface and Atmospheric Climate Change. In M. T. and H. L. M. [(eds.)]. Solomon, S., D. Qin, M. Manning, Z. Chen, M. Marquis, K.B. Averyt (Ed.), *In: Climate Change 2007: The Physical Science Basis. Contribution of Working Group I to the Fourth Assessment Report of the Intergovernmental Panel on Climate Change*. Cambridge University Press, Cambridge, United Kingdom and New York, NY, USA.

Vaughan, D. G., Comiso, J. C., Allison, I., Carrasco, J., Kaser, G., Kwok, R., … Zhang, T. (2013). Observations: Cryosphere. In T. F. Stocker, D. Qin, G.-K. Plattner, M. Tignor, S. K. Allen, V. Boschung, … P. M. Midgley (Eds.), *In: Climate Change 2013: The Physical Science Basis. Contribution of Working Group I to the Fifth Assessment Report of the Intergovernmental Panel on Climate Change*. Cambridge University Press, Cambridge, United Kingdom and New York, NY, USA.

Vicuna, S., & Dracup, J. A. (2007). The evolution of climate change impact studies on hydrology and water resources in California. *Climatic Change*, *82*, 327–350. http://doi.org/10.1007/s10584-006-9207-2

von Storch, H., & Zwiers, F. W. (1999). *Statistical Analysis in Climate Research*. Cambridge University Press.

Westmacott, J. R., & Burn, D. H. (1997). Climate change effects on the hydrologic regime within the Churchill-Nelson River Basin. *Journal of Hydrology*, *202*, 263–279. http://doi.org/10.1016/S0022-1694(97)00073-5

Wildlands, M., & Manitoba Wildlands. (2005). *The Hydro Province : Manitoba's Hydroelectric Complex*.

Wilks, D. S. (2011). *Statistical Methods in the Atmospheric Sciences*. Elsevier Inc.

Zhang, X., Brown, R., Vincent, L., Skinner, W., Feng, Y., & Mekis, E. (2011). *Canadian climate trends, 1950-2007. Canadian Biodiversity: Ecosystem Status and Trends 2010, Technical Thematic Report No. 5*. Retrieved from http://www.biodivcanada.ca/default.asp?lang=En&n=137E1147-0

Zhang, X., Harvey, K. D., Hogg, W. D., & Yuzyk, T. R. (2001). Trends in Canadian streamflow. *Water Resources Research*, *37*(4), 987–998.

Zhao, H., Higuchi, K., Waller, J., Auld, H., & Mote, T. (2013). The impacts of the PNA and NAO on annual maximum snowpack over southern Canada during 1979-2009. *International Journal of Climatology*, *33*, 388–395. http://doi.org/10.1002/joc.3431

Zuur, A. F., Ieno, E. N., & Meesters, E. H. W. G. (2009). *A Beginner's Guide to R*. Springer Science & Business Media. Retrieved from http://books.google.com/books?hl=en&lr=&id=bvwVXHhNQ-4C&oi=fnd&pg=PR3&dq=A+Beginner's+Guide+to+R&ots=nrGHYsD7Xm&sig=F6lCGN-LDf496fioliV_Cq1TDnc

Appendix 1. Average Maximum Snow Depth over Canada (Natural Resources Canada, 2009)

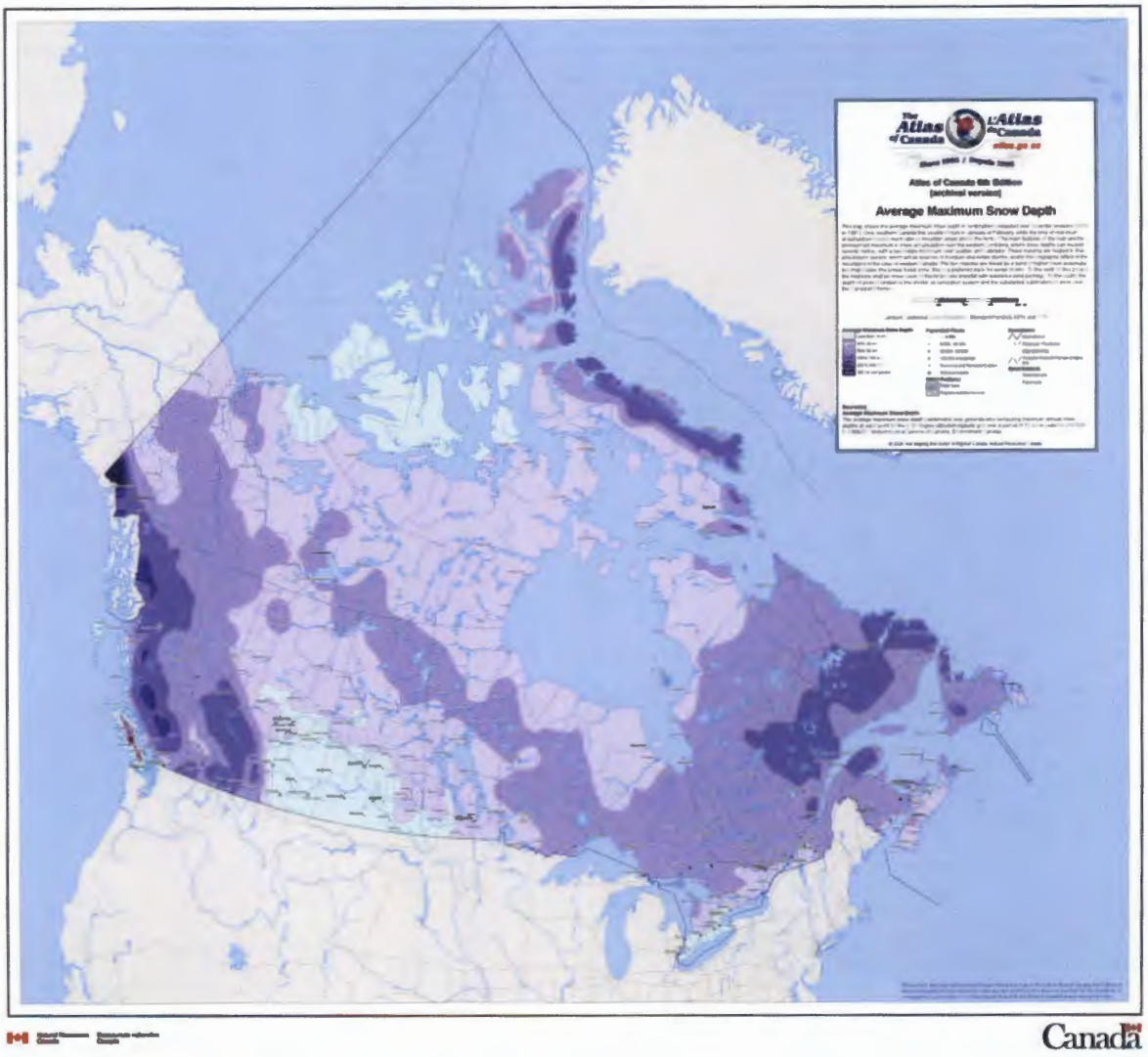

Appendix 2. Annual Mean Total Precipitation over Canada (Natural Resources Canada, 2009)

Appendix 3. List of rivers that include small downstream tributaries

River	Tributaries
Churchill	Deer
Nelson	Angling Limestone Weir
Chesterfield Inlet	Thelon Kazan
Moose	Abitibi Kwataboahegan North French
Winisk	Shamattawa
Harricana	Turgeon